

A generalized uncertainty-inspired quantum black hole

Federica Fragomeno,^a Douglas M. Gingrich,^{a,b} Samantha Hergott,^{c,d}
Saeed Rastgoo,^{a,e,f} Evan Vienneau,^a

^a*Department of Physics, University of Alberta, Edmonton, Alberta T6G 2G1, Canada*

^b*TRIUMF, Vancouver, BC V6T 2A3, Canada*

^c*Department of Physics and Astronomy, York University, Toronto, Ontario M3J 1P3, Canada*

^d*Perimeter Institute for Theoretical Physics, Waterloo, Ontario N2L 2Y5, Canada*

^e*Department of Mathematical and Statistical Sciences, University of Alberta, Edmonton, Alberta T6G 2G1, Canada*

^f*Theoretical Physics Institute, University of Alberta, Edmonton, Alberta T6G 2G1, Canada*

*E-mail: ffragome@ualberta.ca, gingrich@ualberta.ca,
sherrgs@yorku.ca, srastgoo@ualberta.ca, eviennea@ualberta.ca*

ABSTRACT:

We derive the full spacetime metric of a generalized uncertainty-inspired quantum black hole. We examine a previous model of the interior in this approach and show that extending its metric to the full spacetime leads to serious issues in the asymptotic region. To remedy this, we introduce an “improved scheme” mimicking a similar prescription used in loop quantum gravity, where the quantum parameters are made momentum-dependent. Under this scheme, we rework the interior of the black hole and extend it to the full spacetime. We find that the resulting metric is asymptotically flat and its associated Kretschmann scalar is regular everywhere. We also show that the null expansion and Raychaudhuri equation are regular everywhere in this spacetime, implying that the classical singularity is resolved.

Contents

1	Introduction	2
2	Classical Schwarzschild interior in Ashtekar-Barbero variables	4
3	Non-improved effective metric	6
3.1	Non-improved canonical variables and dynamics of the interior	6
3.2	Full spacetime extension of the non-improved metric	8
3.3	Issues with the non-improved extended metric	9
4	Improved effective metric in the $\bar{\beta}$ scheme	10
4.1	Improved metric and its extension to the full spacetime	10
4.2	Classical and asymptotic limits	15
4.3	Spacetime structure, horizon and mass	16
4.4	Kretschmann scalar	19
4.5	Effective stress-energy tensor	21
5	Geodesics	23
5.1	Null geodesics and the photon sphere	24
5.2	Timelike geodesics	24
5.3	Painlevé-Gullstrand coordinates and infalling observers	25
5.3.1	Metric in the Painlevé-Gullstrand coordinates	25
5.3.2	Velocity and proper time of the infalling geodesics	27
5.4	Expansion and Raychaudhuri equation	29
5.4.1	Expansion tensor and scalar	29
5.4.2	Raychaudhuri equation	32
6	Discussion and conclusions	32
A	Equations of motion of the interior	34

1 Introduction

Black holes are considered to be one of the places where new physics can emerge. Thus studying quantum black holes is one of the most important tasks in quantum gravity, in the hope of obtaining hints about the nature of quantum spacetime. This is even more crucial in the age in which there are hopes that several near-future experiments could observe quantum gravity signatures in astrophysical phenomena, particularly from black holes [1–4].

Quantum black holes have been studied in many approaches. In a non-perturbative approach to quantum gravity, called loop quantum gravity (LQG) [5], various models have been put forward. These models are based on a classical phase space with the Ashtekar-Barbero (AB) connection as the configuration variable, and its conjugate momentum the densitized triad. The latter can be thought of as components of the spatial metric. One would then transition to loop classical theory by introducing holonomies of the AB connection as the configuration variable and the flux of densitized triads over 2-surfaces as their momenta. One then quantizes these variables over a suitable Hilbert space. The black hole models in LQG usually follow this process by first symmetry-reducing the classical theory. They include models [6–10] that treat the interior as a Kantowski-Sachs cosmology, the full spacetime [11–16], or further symmetry-reduced 2D systems [17–19]. These models either holonomize or regularize the system as described above using LQG techniques, or use polymer quantization techniques [20–22]. Some of the models follow the procedure without actually quantizing the holonomies and fluxes [11, 13–16], obtaining an “effective” metric just from regularization. Others proceed to quantization and extract the effective metric by obtaining the expectation values of the metric components in certain states that are peaked around classical solutions [12].

Another approach to quantum gravity is the so called generalized uncertainty principle (GUP) approach, sometimes also known as minimal uncertainty approach [23, 24]. This approach is based on the observation that the product of uncertainties in configuration and momenta have a certain relation to the algebra of these variables. Hence, by demanding certain minimal uncertainty in either the configuration or the momenta, the algebra will be modified. This approach has been mostly studied in the case of finite number of degrees of freedom rather than in field theories. Hence, directly applying it to the full spacetime of a black hole is still not well understood. However, this model can be used, and has been used, to study the interior of the Schwarzschild black hole in AB variables, both in the effective regime [25, 26] including a comparison with LQG [27], and in the quantum regime [28].

There have also been several works studying some aspects of black holes in GUP,

particularly their thermodynamics [29–35], and some of them have put forward certain forms of GUP-deformed components of a Schwarzschild-like metric up to the first order in GUP parameters, albeit using heuristic methods [29, 30, 33]. However, to our knowledge, there have been no systematic derivations of a full GUP metric (i.e., not perturbatively up to a certain order in GUP parameters, and not solely based on heuristic arguments) until now. This is where our work fills the gap.

In this work, we derive the full spacetime metric of a GUP-modified Schwarzschild black hole using a combination of techniques from both GUP and LQG. To avoid dealing with the full spacetime directly, which is a field theory, we start by treating the interior written in AB variables using a GUP-modified algebra. Then we extend the resulting metric of the interior to the full spacetime. This is similar to the approach used in some of the proposed models in LQG [13, 14, 36]. However, the resulting metric suffers from some of the asymptotic issues encountered in [13] and discussed further in [37, 38]. In order to remedy these issues, we follow the “improved prescriptions” in LQG by making the quantum parameters of the model, which were originally constant, momentum-dependent. Remarkably this prescription not only resolves the asymptotic issues but renders the black hole regular.

The order of material in this work is as follows. In Sec. 2 we present a brief overview of the dynamics of the interior of the Schwarzschild black hole in AB variables. In Sec. 3 we show how the GUP treatment of the interior without considering momentum-dependent quantum parameters, leads to a full spacetime metric and a Kretschmann scalar with asymptotic issues. Sec. 4 is dedicated to reworking the interior with the improved GUP approach (where the modifications to the algebra are made momentum dependent to obtain an improved version in which the classical and asymptotic limits are correct), extending it to the full spacetime, and showing that not only this metric has all the desired asymptotic properties, but also its Kretschmann scalar is regular everywhere. We also work out some of the properties of this metric including the effective stress-energy tensor, obtained if we would assume Einstein’s equations are valid. In Sec. 5 we study several properties of geodesics in this spacetime, including the photon spheres, the velocity of the infalling observer, and more importantly, the expansion scalar and the Raychaudhuri equation. We argue that all these results point to the resolution of the classical singularity which is demonstrated by showing that the expansion scalar and the Raychaudhuri equation are regular everywhere. Finally, in Sec. 6, we summarize our results and make some concluding remarks.

2 Classical Schwarzschild interior in Ashtekar-Barbero variables

We begin by reviewing the interior solution for a Schwarzschild black hole in Ashtekar-Barbero variables. The interior of a static spherically symmetric black hole in Ashtekar-Barbero variables in Schwarzschild coordinates can be described by the metric [6]

$$d\tilde{s}^2 = -\tilde{N}(\tilde{T})^2 d\tilde{T}^2 + \frac{\tilde{p}_b^2(\tilde{T})}{L_0^2 |\tilde{p}_c(\tilde{T})|} d\tilde{r}^2 + |\tilde{p}_c(\tilde{T})| \left(d\tilde{\theta}^2 + \sin^2(\tilde{\theta}) d\tilde{\phi}^2 \right), \quad (2.1)$$

where tilde symbols refer to the interior coordinates and variables, and \tilde{T} is timelike and \tilde{r} is spacelike in the interior. The function \tilde{N} is the lapse function arising due to the ADM (Arnowitt-Deser-Misner) decomposition of the interior spacetime. The timelike coordinate \tilde{T} is a generic one that is associated with the choice of \tilde{N} , and is generally not the timelike coordinate of the Schwarzschild interior metric which we call \tilde{t} . The variables \tilde{b} , \tilde{c} , \tilde{p}_b and \tilde{p}_c are the components of the Ashtekar-Barbero connection A_a^i and the densitized triad \mathcal{E}_i^a , respectively [6], adapted to the symmetry of the model:

$$A_a^i \tau_i d\tilde{x}^a = \frac{\tilde{c}}{L_0} \tau_3 d\tilde{r} + \tilde{b} \tau_2 d\tilde{\theta} - \tilde{b} \tau_1 \sin(\tilde{\theta}) d\tilde{\phi} + \tau_3 \cos(\tilde{\theta}) d\tilde{\phi}, \quad (2.2)$$

$$\mathcal{E}_i^a \tau_i \partial_a = \tilde{p}_c \tau_3 \sin(\tilde{\theta}) \partial_{\tilde{r}} + \frac{\tilde{p}_b}{L_0} \tau_2 \sin(\tilde{\theta}) \partial_{\tilde{\theta}} - \frac{\tilde{p}_b}{L_0} \tau_1 \partial_{\tilde{\phi}}. \quad (2.3)$$

Hence, \tilde{b} and \tilde{c} are the configuration variables, and \tilde{p}_b and \tilde{p}_c are their associated conjugate momenta. Here L_0 is a fiducial parameter introduced to make the symplectic structure, and hence the definition of the Poisson brackets, well-defined. Clearly, no physical observables should depend on L_0 or on its rescaling. The τ_i are the basis of the $su(2)$, and i is an $SU(2)$ index, while a is a spatial index. The algebra of canonical variables, inherited from the algebra of A_a^i and \mathcal{E}_i^a , is

$$\{\tilde{b}, \tilde{p}_b\} = G\gamma \quad \text{and} \quad \{\tilde{c}, \tilde{p}_c\} = 2G\gamma, \quad (2.4)$$

where γ is the Barbero-Immirzi parameter [5], which is a free parameter in loop quantum gravity that is taken to be real and positive, and can be fixed by, for example, computations of black hole entropy. The classical Hamiltonian (constraint) under the relevant symmetry reduction of this model becomes [6]

$$\tilde{H} = -\frac{\tilde{N} \text{sgn}(\tilde{p}_c)}{2G\gamma^2} \left[\left(\tilde{b}^2 + \gamma^2 \right) \frac{\tilde{p}_b}{\sqrt{|\tilde{p}_c|}} + 2\tilde{b}\tilde{c}\sqrt{|\tilde{p}_c|} \text{sgn}(\tilde{p}_c) \right]. \quad (2.5)$$

The classical Hamiltonian equations of motion $f = \{f, H\}$ for \tilde{c} and \tilde{p}_c can be decoupled from those of \tilde{b} and \tilde{p}_b by choosing the lapse

$$\tilde{N}(\tilde{T}) = \frac{\gamma \operatorname{sgn}(\tilde{p}_c) \sqrt{|\tilde{p}_c(\tilde{T})|}}{\tilde{b}(\tilde{T})}, \quad (2.6)$$

which reduces the Hamiltonian to

$$\tilde{H} = -\frac{1}{2G\gamma} \left[(\tilde{b}^2 + \gamma^2) \frac{\tilde{p}_b}{\tilde{b}} + 2\tilde{c}\tilde{p}_c \right]. \quad (2.7)$$

Solving these equations of motion yield

$$\tilde{b}(\tilde{T}) = \pm \sqrt{e^{2C_1} e^{-\tilde{T}} - \gamma^2}, \quad (2.8)$$

$$\tilde{p}_b(\tilde{T}) = C_2 e^{\frac{\tilde{T}}{2}} \sqrt{e^{2C_1} - \gamma^2 e^{\tilde{T}}}, \quad (2.9)$$

$$\tilde{c}(\tilde{T}) = \mp C_3 e^{-2\tilde{T}}, \quad (2.10)$$

$$\tilde{p}_c(\tilde{T}) = \pm C_4 e^{2\tilde{T}}. \quad (2.11)$$

To fix the integration constants, we can compare the spatial components of the metric (2.1) with the Schwarzschild interior metric:

$$\frac{\tilde{p}_b^2(\tilde{T})}{L_0^2 \tilde{p}_c(\tilde{T})} = g_{rr}(\tilde{t}) = \left(\frac{2GM}{\tilde{t}} - 1 \right), \quad (2.12)$$

$$\tilde{p}_c(\tilde{T}) = g_{\theta\theta}(\tilde{t}) = \frac{g_{\phi\phi}(\tilde{t})}{\sin^2(\tilde{\theta})} = \tilde{t}^2. \quad (2.13)$$

We see that to match (2.13) and (2.11), we need a coordinate transformation $\tilde{T} = \ln(\tilde{t})$ and a choice of $C_4 = 1$ (or $C_4 = -1$ for the negative solution of \tilde{p}_c). Notice that this means $\tilde{t} = 0$ is not part of the manifold. This also means that in Schwarzschild coordinates $(\tilde{t}, \tilde{r}, \tilde{\theta}, \tilde{\phi})$, the general spherically symmetric metric corresponding to (2.1) is

$$d\tilde{s}^2 = -\frac{\tilde{N}(\tilde{t})^2}{\tilde{t}^2} d\tilde{t}^2 + \frac{\tilde{p}_b^2(\tilde{t})}{L_0^2 \tilde{p}_c(\tilde{t})} d\tilde{r}^2 + \tilde{p}_c(\tilde{t}) \left(d\tilde{\theta}^2 + \sin^2(\tilde{\theta}) d\tilde{\phi}^2 \right). \quad (2.14)$$

The remainder of the integration constants in (2.8)-(2.10) can be found by considering $\tilde{p}_b(\tilde{t} = 2GM) = 0$ and by matching (2.12) to the solutions – all after the coordinate transformation $\tilde{T} = \ln(\tilde{t})$. Then the classical solutions in the Schwarzschild interior

coordinates become

$$\tilde{b}(\tilde{t}) = \gamma \sqrt{\frac{R_s}{\tilde{t}} - 1}, \quad (2.15)$$

$$\tilde{p}_b(\tilde{t}) = L_0 \tilde{t} \sqrt{\frac{R_s}{\tilde{t}} - 1}, \quad (2.16)$$

$$\tilde{c}(\tilde{t}) = -\frac{\gamma L_0 R_s}{2\tilde{t}^2}, \quad (2.17)$$

$$\tilde{p}_c(\tilde{t}) = \tilde{t}^2, \quad (2.18)$$

where $R_s = 2GM$ is the Schwarzschild radius.

In the classical regime, the Kretschmann scalar in variables (2.15)-(2.18) becomes

$$K_{\text{class}} = \frac{12 \left(\tilde{b}^2 + \gamma^2 \right)^2}{\gamma^4 \tilde{p}_c^2}. \quad (2.19)$$

Notice that $|\tilde{p}_c|$ is the square of the radius of 2-spheres in these coordinates. The Kretschmann scalar above clearly diverges for $\tilde{p}_c \rightarrow 0$, which is the position where the classical singularity resides.

3 Non-improved effective metric

3.1 Non-improved canonical variables and dynamics of the interior

We are now going to implement modifications to the Poisson algebra according to the GUP approach [23, 24] by choosing a quadratic modification in configuration variables as

$$\{b, p_b\} = G\gamma (1 + \beta_b b^2), \quad (3.1)$$

$$\{c, p_c\} = 2G\gamma (1 + \beta_c c^2), \quad (3.2)$$

where β_b and β_c are small dimensionless parameters, also known as GUP parameters.

The GUP approach is based on the observation that the uncertainty in the configuration variable q and its conjugate momentum p , is related to their algebra via

$$\Delta q \Delta p \geq \frac{\hbar}{2} | \langle [\hat{q}, \hat{p}] \rangle |. \quad (3.3)$$

Therefore a modification to the algebra such as

$$[\hat{q}, \hat{p}] = i\hbar (1 + \beta \langle q^2 \rangle + \alpha \langle p^2 \rangle) \quad (3.4)$$

leads to a modified uncertainty relation [23, 24]

$$\Delta q \Delta p \geq \frac{\hbar}{2} [1 + \beta(\Delta q)^2 + \alpha(\Delta p)^2 + \beta \langle q \rangle^2 + \alpha \langle p \rangle^2]. \quad (3.5)$$

This in turn implies the existence of a minimal uncertainty in both q and p , given that $\alpha > 0$ and $\beta > 0$ [23, 24]. Applied to the gravitational variables as we have done above, it leads to a minimal uncertainty in the momenta which are the components of the triad, and ultimately the metric. So given that $\beta > 0$, this modification of algebra leads to some sort of minimum value associated to the metric.

This approach however, will encounter several issues if it is only restricted to positive deformation parameters α and β . Some of the well-know issues are the followings. Positive deformation parameters result in the Chandrasekhar limit no longer existing, thus making arbitrarily large white dwarfs allowed [34, 39, 40]. The computation of temperature of the Hawking radiation could lead to negative deformation parameters [29, 30, 35]. Furthermore, in a systematic study of the interior dynamics, the only way to remove the singularity seems to enforce the negative sign on the deformation parameters [25–27]. Finally an analysis based on horizon quantum mechanics also leads to the fact that these GUP parameters should be negative [31].

If one extends this method, particularly (3.4), to negative values of GUP parameters, one will not obtain a minimal uncertainty anymore, but the aforementioned issues will be resolved. The negativity of deformation parameters hints that the physical space-time has actually a lattice or granular structure at the Planck scale, essentially a crystal-like universe whose lattice spacing is of the order of Planck length [32]. We will discuss the particular case of our model in more detail at the end of Sec. 4.1.

Although (3.1) and (3.2) do not modify the Hamiltonian, they lead to effective equations of motion that are different from the classical ones due to modification to the Poisson algebra (see appendix A). The solution to these modified equations of motion are [25–27]

$$\tilde{b} = \frac{\gamma \sqrt{R_s t^{\beta_b \gamma^2} - t (\gamma^2 R_s)^{\beta_b \gamma^2}}}{\sqrt{t (\gamma^2 R_s)^{\beta_b \gamma^2} - \beta_b \gamma^2 R_s t^{\beta_b \gamma^2}}}, \quad (3.6)$$

$$\tilde{p}_b = \gamma L_0 t^{-\beta_b \gamma^2} \sqrt{R_s t^{\beta_b \gamma^2} - t (\gamma^2 R_s)^{\beta_b \gamma^2}} \sqrt{t (\gamma^2 R_s)^{\beta_b \gamma^2} - \beta_b \gamma^2 R_s t^{\beta_b \gamma^2}}, \quad (3.7)$$

$$\tilde{c} = - \frac{\gamma L_0 R_s}{2 \sqrt{t^4 - \frac{1}{4} \beta_c \gamma^2 L_0^2 R_s^2}}, \quad (3.8)$$

$$\tilde{p}_c = \sqrt{t^4 - \frac{1}{4} \beta_c \gamma^2 L_0^2 R_s^2}. \quad (3.9)$$

The constants of integration in these solutions have been fixed by matching the classical limit of these solutions when $\beta_b \rightarrow 0$ and $\beta_c \rightarrow 0$, with the actual classical solutions (2.15)-(2.18). Replacing the solutions into the metric (2.14) together with (2.6) (written in \tilde{t}) yields the effective interior metric.

3.2 Full spacetime extension of the non-improved metric

Since the extended (interior and exterior) metric of the classical Schwarzschild spacetime can be derived by switching the timelike and spacelike coordinates of the Schwarzschild interior, as a first attempt, we try to apply the same concept to the interior metric in the GUP approach to obtain the full spacetime metric. In other words, we switch $\tilde{t} \rightarrow r$ and $\tilde{r} \rightarrow t$ (and for consistency in notation $\tilde{\theta} \rightarrow \theta$ and $\tilde{\phi} \rightarrow \phi$) in the solutions (3.6)-(3.9) and in the metric (2.14). Note that since we mentioned before that $\tilde{t} = 0$ is not part of the manifold, the aforementioned switch means now $r = 0$ is not part of the manifold. The extended (interior and exterior) spacetime metric is now

$$ds^2 = \frac{\check{p}_b^2(r)}{L_0^2 \check{p}_c(r)} dt^2 - \frac{1}{r^2} \frac{\gamma^2 \check{p}_c(r)}{\check{b}^2(r)} dr^2 + \check{p}_c(r) (d\theta^2 + \sin^2(\theta) d\phi^2), \quad (3.10)$$

where we have denoted the extended canonical variables by check symbols. From now on we will consider both interior and exterior as described by coordinates (t, r, θ, ϕ) , and keep in mind that t and r are timelike and spacelike in the exterior, respectively, and spacelike and timelike in the interior, respectively.

In order to write the canonical variables (3.6)-(3.9) and the full spacetime metric in a concise way, we define the following quantities

$$\check{Q}_b = |\beta_b| \gamma^2, \quad (3.11)$$

$$\check{Q}_c = |\beta_c| \gamma^2, \quad (3.12)$$

and

$$\check{\lambda}(r) = r (\gamma^2 R_s)^{\text{sgn}(\beta_b) \check{Q}_b} - R_s r^{\text{sgn}(\beta_b) \check{Q}_b}, \quad (3.13)$$

$$\check{\mu}(r) = r (\gamma^2 R_s)^{\text{sgn}(\beta_b) \check{Q}_b} - \text{sgn}(\beta_b) \check{Q}_b R_s r^{\text{sgn}(\beta_b) \check{Q}_b}, \quad (3.14)$$

$$\check{\xi}(r) = 4r^4 - L_0^2 \text{sgn}(\beta_c) \check{Q}_c R_s^2. \quad (3.15)$$

Then the canonical variables can be expressed as

$$\check{b}(r) = \gamma \sqrt{-\frac{\check{\lambda}(r)}{\check{\mu}(r)}}, \quad (3.16)$$

$$\check{p}_b(r) = \frac{L_0}{r^{\text{sgn}(\beta_b)\check{Q}_b}} \sqrt{-\check{\lambda}(r)\check{\mu}(r)}, \quad (3.17)$$

$$\check{c}(r) = -\frac{\gamma L_0 R_s}{\sqrt{\check{\xi}(r)}}, \quad (3.18)$$

$$\check{p}_c(r) = \frac{1}{2} \sqrt{\check{\xi}(r)}. \quad (3.19)$$

Replacing these expressions for the components of the extended metric (3.10) yields the metric components

$$\check{g}_{00} = \frac{\check{p}_b^2}{L_0^2 \check{p}_c} = -\frac{2}{r^{2\text{sgn}(\beta_b)\check{Q}_b}} \frac{\check{\lambda}(r)\check{\mu}(r)}{\sqrt{\check{\xi}(r)}}, \quad (3.20)$$

$$\check{g}_{11} = -\frac{\gamma^2 \check{p}_c}{\check{b}^2 r^2} = \frac{1}{2r^2} \sqrt{\check{\xi}(r)} \frac{\check{\mu}(r)}{\check{\lambda}(r)}, \quad (3.21)$$

$$\check{g}_{22} = \frac{\check{g}_{33}}{\sin^2(\theta)} = \frac{1}{2} \sqrt{\check{\xi}(r)}. \quad (3.22)$$

Note that in order to get the correct signature for the metric, we need $\check{\lambda}$ and $\check{\mu}$ to have the same sign which means that, similar to some of the approaches in LQG [37], \check{b} and \check{p}_b are imaginary in the exterior.

3.3 Issues with the non-improved extended metric

The full spacetime metric described by (3.20)-(3.22) should have correct classical as well as asymptotic limits. It can be seen that although the classical limits are fine:

$$\lim_{\beta_b, \beta_c \rightarrow 0} \bar{g}_{00} = -\left(1 - \frac{R_s}{r}\right), \quad (3.23)$$

$$\lim_{\beta_b, \beta_c \rightarrow 0} \bar{g}_{11} = \left(1 - \frac{R_s}{r}\right)^{-1}, \quad (3.24)$$

$$\lim_{\beta_b, \beta_c \rightarrow 0} \bar{g}_{22} = r^2. \quad (3.25)$$

The asymptotic limits are incorrect,

$$\lim_{r \rightarrow \infty} \bar{g}_{00} = \begin{cases} 0, & \text{sgn}(\beta_b) = 1 \\ -\infty, & \text{sgn}(\beta_b) = -1 \end{cases}, \quad (3.26)$$

$$\lim_{r \rightarrow \infty} \bar{g}_{11} = \begin{cases} \check{Q}_b, & \text{sgn}(\beta_b) = 1 \\ 1, & \text{sgn}(\beta_b) = -1 \end{cases}. \quad (3.27)$$

Furthermore, the asymptotic expansion of the Kretschmann scalar also falls off incorrectly as $K \propto r^{-4}$. This situation is similar to [37] where in addition to the issue with the fall-off of the Kretschmann scalar in the asymptotic region, this region is not maximally symmetric, and furthermore, e.g., surfaces that should be null in the asymptotic region, do not have this caudal structure [38].

In LQG, certain prescriptions are applied to resolve similar issues by making the quantum parameters of the models momentum-dependent (or scale factor-dependent in Bianchi models) [8, 41, 42]. These prescriptions are collectively known as improved schemes. Usually the term “improved” in this context refers to a scheme that leads to the correct classical and asymptotic limits and also removes large quantum gravity effects from low curvature regions. Inspired by these methods, we will apply a similar prescription to the model at hand.

4 Improved effective metric in the $\bar{\beta}$ scheme

4.1 Improved metric and its extension to the full spacetime

As mentioned at the end of the previous section, we are now going to make the quantum parameters β_b and β_c momentum-dependent. This is done by modifying the dimensionless quantum parameters to

$$\beta_b \rightarrow \bar{\beta}_b = \frac{\beta_b L_0^4}{p_b^2}, \quad (4.1)$$

$$\beta_c \rightarrow \bar{\beta}_c = \frac{\beta_c L_0^4}{p_c^2}, \quad (4.2)$$

where the powers of L_0 are included to render the $\bar{\beta}$'s dimensionless. We call this prescription the $\bar{\beta}$ improved scheme after a similar method used in LQG [8, 41, 42]. As a result of the above, the effective GUP-induced algebra now becomes

$$\{b, p_b\} = G\gamma (1 + \bar{\beta}_b b^2) = G\gamma \left(1 + \frac{\beta_b L_0^4}{p_b^2} b^2 \right), \quad (4.3)$$

$$\{c, p_c\} = 2G\gamma (1 + \bar{\beta}_c c^2) = 2G\gamma \left(1 + \frac{\beta_c L_0^4}{p_c^2} c^2 \right). \quad (4.4)$$

Note that this is done at the level of the Poisson algebra, before solving the equations of motion in the interior. Hence, we need to rework the entire interior dynamics with the same Hamiltonian as (2.7), but using the improved algebra (4.3)-(4.4). As we will see, this modification remarkably resolves the asymptotic issues that arose in the extension of the metric to the full spacetime in the previous section, and furthermore leads to

the singularity resolution in this black hole as we will see in the following sections. By singularity resolution we mean four things: finiteness of Riemann invariants everywhere in the spacetime, geodesic completeness, finiteness of both the expansion scalar and the Raychaudhuri equation, and nonvanishing of the radius of 2-spheres. We will present these results gradually in relevant sections in what follows.

Solving the equations of motion (see appendix A) and fixing the integration constants by matching the classical limits, $\beta_b \rightarrow 0$ and $\beta_c \rightarrow 0$, of the canonical variables with the actual classical solutions (2.15)-(2.18) of the interior, results in

$$b = \gamma \sqrt{\frac{-\left(\tilde{t}^2 - \text{sgn}(\beta_b) Q_b\right) + R_s \sqrt{\tilde{t}^2 - \text{sgn}(\beta_b) Q_b}}{\tilde{t}^2 - \text{sgn}(\beta_b) Q_b}}, \quad (4.5)$$

$$p_b = L_0 \sqrt{\tilde{t}^2 - \text{sgn}(\beta_b) Q_b} \sqrt{\frac{-\left(\tilde{t}^2 - \text{sgn}(\beta_b) Q_b\right) + R_s \sqrt{\tilde{t}^2 - \text{sgn}(\beta_b) Q_b}}{\tilde{t}^2 - \text{sgn}(\beta_b) Q_b}}, \quad (4.6)$$

$$c = -\frac{\gamma L_0 R_s}{2 \left(\tilde{t}^8 - \frac{1}{4} \text{sgn}(\beta_c) Q_c R_s^2\right)^{\frac{1}{4}}}, \quad (4.7)$$

$$p_c = \left(\tilde{t}^8 - \frac{1}{4} \text{sgn}(\beta_c) Q_c R_s^2\right)^{\frac{1}{4}}. \quad (4.8)$$

In the above, we have defined two positive dimensionful quantum parameters

$$Q_b = |\beta_b| \gamma^2 L_0^2 \quad \text{and} \quad Q_c = |\beta_c| \gamma^2 L_0^6, \quad (4.9)$$

where Q_b has dimensions of $[L]^2$ and Q_c has dimensions of $[L]^6$.

Once again, we are going to postulate that, just as in the standard classical Schwarzschild case, the full spacetime metric of this GUP-inspired black hole is derived by analytical extension of the interior by switching $\tilde{t} \rightarrow r$, $\tilde{r} \rightarrow t$, $\tilde{\theta} \rightarrow \theta$ and $\tilde{\phi} \rightarrow \phi$, where t and r are the usual Schwarzschild coordinates. To obtain the full spacetime metric in this way we make the aforementioned switch of coordinate labels in (4.5)-(4.8), and obtain the extended version of the canonical variables as

$$b = \gamma \sqrt{\frac{R_s}{\sqrt{\nu}} - 1}, \quad (4.10)$$

$$p_b = L_0 \sqrt{\nu} \sqrt{\frac{R_s}{\sqrt{\nu}} - 1}, \quad (4.11)$$

$$c = -\frac{\gamma L_0 R_s}{2 \rho^{\frac{1}{4}}}, \quad (4.12)$$

$$p_c = \rho^{\frac{1}{4}}. \quad (4.13)$$

Here we have defined

$$\nu = r^2 - \text{sgn}(\beta_b) Q_b \quad \text{and} \quad \rho = r^8 - \frac{1}{4} \text{sgn}(\beta_c) Q_c R_s^2. \quad (4.14)$$

Replacing the solutions (4.10)-(4.13) into the full spacetime metric

$$ds^2 = -\frac{1}{r^2} \frac{\gamma^2 p_c(r)}{b^2(r)} dr^2 + \frac{p_b^2(r)}{L_0^2 p_c(r)} dt^2 + p_c(r) (d\theta^2 + \sin^2(\theta) d\phi^2), \quad (4.15)$$

we obtain the improved full metric components

$$g_{00} = \frac{p_b^2}{L_0^2 p_c} = -\sqrt{\frac{\nu}{\sqrt{\rho}}} (\sqrt{\nu} - R_s), \quad (4.16)$$

$$g_{11} = -\frac{\gamma^2 p_c}{b^2 r^2} = \frac{\sqrt{\nu} \sqrt{\rho}}{r^2 (\sqrt{\nu} - R_s)}, \quad (4.17)$$

$$g_{22} = \frac{g_{33}}{\sin^2(\theta)} = \rho^{\frac{1}{4}}. \quad (4.18)$$

Before continuing, let us briefly examine the signature and the conditions on reality of the above metric. To have a metric which remains real for all values of coordinates, particularly for all values of $r \in (0, \infty)$, we need both ν and ρ to always remain non-negative. As a result, from (4.14) and (4.9) we infer

$$\nu > 0 \Rightarrow \text{sgn}(\beta_b) = -1, \quad (4.19)$$

$$\rho > 0 \Rightarrow \text{sgn}(\beta_c) = -1. \quad (4.20)$$

This is the same result that had been obtained in previous works regarding the interior of this black hole [25–28]. This choice of the signs turns (4.9) into

$$Q_b = \beta_b \gamma^2 L_0^2, \quad (4.21)$$

$$Q_c = \beta_c \gamma^2 L_0^6, \quad (4.22)$$

and accordingly we rewrite (4.14) as

$$\nu = r^2 + Q_b, \quad (4.23)$$

$$\rho = r^8 + \frac{1}{4} Q_c R_s^2. \quad (4.24)$$

With the conditions (4.19)-(4.20), not only the reality of the metric for all $r \in (0, \infty)$ is guaranteed, but also its signature would be the expected one for both the interior and the exterior. With these considerations, a plot of the canonical variables (4.10)-(4.13) is shown in Fig. 1. From (4.18) and (4.24) (and Fig. 1), one can see as $r \rightarrow 0$, the

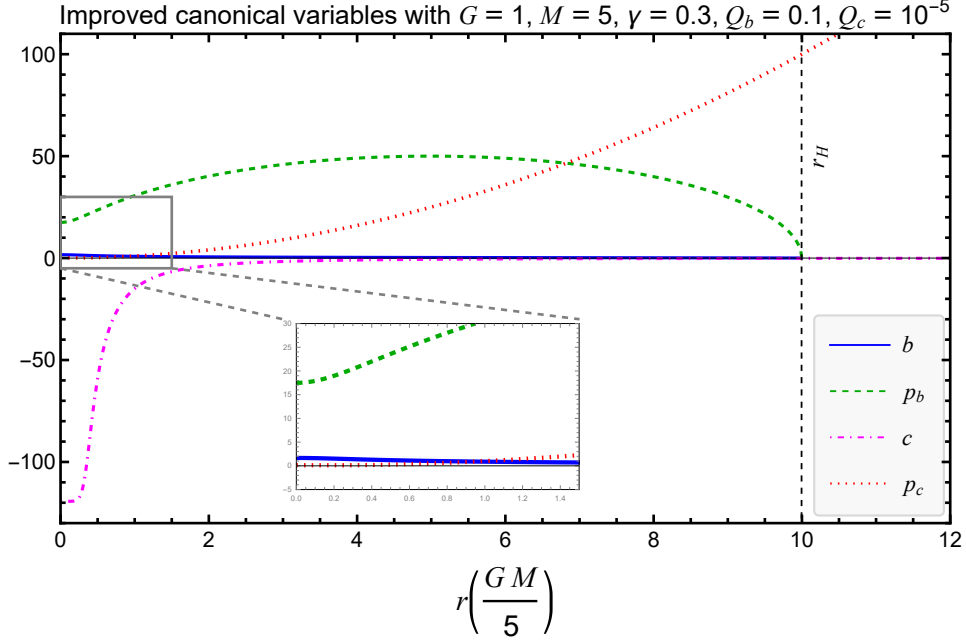


Figure 1. Plot of improved canonical variables with the given values of parameters on the top of the plot. Notice that both b and p_b become imaginary in the exterior. The horizon radius is r_H .

square of the radius of 2-spheres $g_{22} = p_c$ will not vanish. Although not a proof, but given the form of the Kretschmann scalar (2.19) with p_c in the denominator, this already signals we are moving in the right direction with regard to the resolution of the classical singularity.

Hence, the final expression for the improved full spacetime metric components are (4.16)-(4.18) together with (4.23)-(4.24), and (4.21)-(4.22), which are explicitly written as

$$\begin{aligned}
 g_{00} &= -\sqrt{\frac{\nu}{\sqrt{\rho}}} (\sqrt{\nu} - R_s) \\
 &= -\left(1 + \frac{Q_b}{r^2}\right) \left(1 + \frac{Q_c R_s^2}{4r^8}\right)^{-1/4} \left(1 - \frac{R_s}{\sqrt{r^2 + Q_b}}\right), \tag{4.25}
 \end{aligned}$$

$$g_{11} = \frac{\sqrt{\nu}\sqrt{\rho}}{r^2(\sqrt{\nu} - R_s)} = \left(1 + \frac{Q_c R_s^2}{4r^8}\right)^{1/4} \left(1 - \frac{R_s}{\sqrt{r^2 + Q_b}}\right)^{-1}, \tag{4.26}$$

$$g_{22} = \frac{g_{33}}{\sin^2(\theta)} = \rho^{1/4} = r^2 \left(1 + \frac{Q_c R_s^2}{4r^8}\right)^{1/4}. \tag{4.27}$$

The coordinates have the natural domain $r \in [0, +\infty)$, $t \in (-\infty, +\infty)$, $\theta \in [0, \pi]$ and

$\phi \in [0, 2\pi]$. A plot of these metric components are presented in Fig. 2. The existence of the minimum radius of 2-spheres is related to the resolution of the singularity and we see that the quantum effects close to the singularity are associated to β_c as expected.

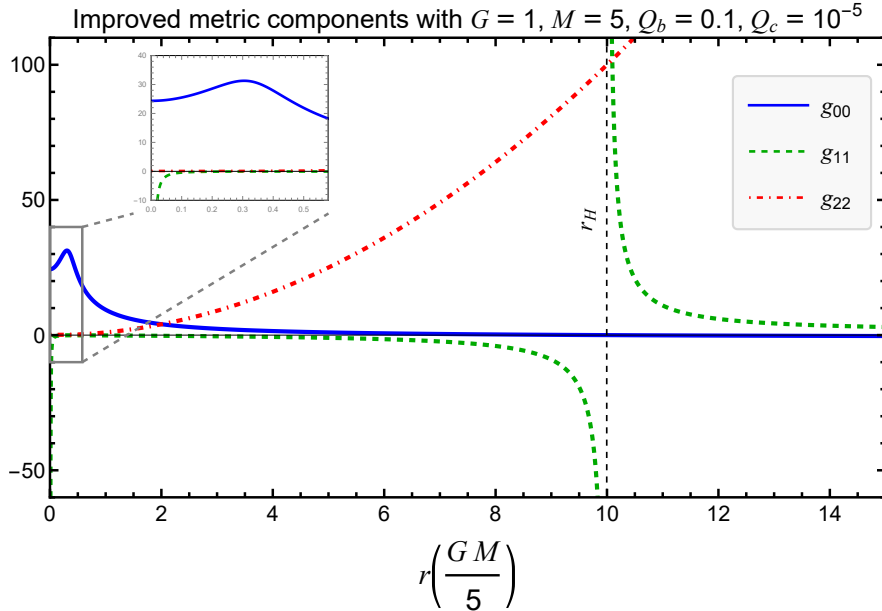


Figure 2. Plot of improved metric components in Schwarzschild coordinates with the given values of parameters on the top of the plot. Note the divergence of g_{11} at $r = 0$.

The above metric components depend on three real non-zero positive parameters: M , Q_b and Q_c . As we will see later in detail in Sec. 4.3, certain relations between these three parameters lead to three types of spacetimes: a black hole, a wormhole, or a remnant.

Before moving on to the properties of this metric we would like to briefly discuss the consequences of Eqs. (4.19) and (4.20). The negativity of β_b , β_c does not allow the existence of minimal uncertainty. This means that the theory is in the regime of generalized uncertainty instead. As discussed in [32], if such a model is considered in the realm of quantum mechanics where X is the position operator with eigenvalues x , and P is the momentum operator with eigenvalues p , and a version of generalized uncertainty is used where p is on the right hand side of the commutators multiplied by β , then this leads to a crystal-like universe where there is a lattice in x with a lattice spacing of the order of Planck length. Furthermore, for energies that are near the border of the Brillouin zone, in this case Planckian energies, the uncertainty relation for position and momenta does not pose any lower bound on uncertainties.

In our case, there are two main differences from the above treatment: 1) our algebra is not on points of space x and their momenta, since in general relativity these points have no physical meaning due to diffeomorphism invariance. Instead, the fundamental algebra that is modified is the algebra of the metric (or equivalently triads) and its conjugate. 2) In our model, the variable on the right hand side of the Poisson bracket multiplied by $\bar{\beta}$'s is not the momentum but the configuration variable (components of the Ashtekar-Barbero connection). One then expects that the lattice behavior is now associated to the triads or the metric. This very much makes sense since if triads can only take certain discrete values, one is dealing with a discrete metric and consequently a quantum spacetime.

4.2 Classical and asymptotic limits

It is quite easy to see that the classical limit $\beta_b \rightarrow 0$ and $\beta_c \rightarrow 0$ (or equivalently $Q_b \rightarrow 0$ and $Q_c \rightarrow 0$ according to (4.21)-(4.22)) of the improved metric components (4.25)-(4.27) match those of the classical Schwarzschild metric; explicitly

$$\lim_{\beta_b, \beta_c \rightarrow 0} g_{00} = - \left(1 - \frac{R_s}{r}\right), \quad \lim_{\beta_b, \beta_c \rightarrow 0} g_{11} = \left(1 - \frac{R_s}{r}\right)^{-1}, \quad \lim_{\beta_b, \beta_c \rightarrow 0} g_{22} = r^2. \quad (4.28)$$

For the asymptotic limit, we have

$$\lim_{r \rightarrow \infty} g_{00} = -1, \quad \lim_{r \rightarrow \infty} g_{11} = 1, \quad \lim_{r \rightarrow \infty} g_{22} = \infty. \quad (4.29)$$

This improved prescription fixes the issues with the asymptotic limit and the asymptotic expansion of the metric. The asymptotic expansions also match the Schwarzschild spacetime to leading order:

$$g_{00}|_{r \rightarrow \infty} = - \left(1 - \frac{R_s}{r}\right) - \frac{Q_b}{r^2} + \mathcal{O}\left(\frac{1}{r}\right)^3, \quad (4.30)$$

$$g_{11}|_{r \rightarrow \infty} = \left(1 + \frac{R_s}{r}\right) + \frac{R_s^2}{r^2} + \frac{R_s}{2r^3} (2R_s^2 - Q_b) + \mathcal{O}\left(\frac{1}{r}\right)^4, \quad (4.31)$$

$$g_{22}|_{r \rightarrow \infty} = r^2 + \frac{Q_c R_s^2}{16r^6} + \mathcal{O}\left(\frac{1}{r}\right)^{14}. \quad (4.32)$$

Notice that as expected from previous studies, the asymptotic and large r behavior is governed by β_b . On the other hand the singularity resolution is governed by β_c as we will see in the next section.

4.3 Spacetime structure, horizon and mass

Since the model is static and spherically symmetric, the event horizon is a Killing horizon, and we can obtain the position of the event horizon simply by solving either $g^{11}(r_H) = 0$ (for event horizons) or $g_{00}(r_H) = 0$ (for Killing horizons corresponding to the asymptotic timelike Killing vector field). This yields the horizon radius as

$$r_H = \sqrt{R_s^2 - Q_b} = R_s \sqrt{1 - \frac{Q_b}{R_s^2}}, \quad (4.33)$$

which is smaller than the Schwarzschild radius, albeit by a very small amount. As should be clear, this is a pure quantum effect. Up to the first order in Q_b we have

$$r_H = R_s - \frac{1}{2} \frac{Q_b}{R_s} + \mathcal{O}\left(\frac{Q_b^2}{R_s^3}\right). \quad (4.34)$$

Given the solution for the horizon, different spacetimes are possible depending on the relative values of M and Q_b . To see this better, let us first make a transformation

$$\bar{r}^8 = r^8 + \frac{1}{4} Q_c R_s^2 \quad (4.35)$$

such that in the new coordinate system $g_{22} = \bar{r}^2$. Notice that now the minimum radius of 2-spheres is

$$\bar{r}_{\min} = \bar{r}(r = 0) = \left(\frac{1}{4} Q_c R_s^2\right)^{\frac{1}{8}}. \quad (4.36)$$

Furthermore, in this new coordinate system, the position of the horizon becomes

$$\begin{aligned} \bar{r}_H^8 &= r_H^8 + \frac{1}{4} Q_c R_s^2 \\ &= (R_s^2 - Q_b)^4 + \frac{1}{4} Q_c R_s^2, \end{aligned} \quad (4.37)$$

where we have used (4.33). Now we will have three cases. For $\bar{r}_H > \bar{r}_{\min}$, or equivalently

$$(R_s^2 - Q_b)^4 > 0 \Rightarrow M > \frac{\sqrt{Q_b}}{2G}, \quad (4.38)$$

the spacetime exhibits an event horizon (two solutions for $g^{11} = 0$, one with a positive r value and one with a negative r value, or the equivalent in the \bar{r} coordinate system) and is thus a black hole. This is confirmed by an analysis of the trapped region of the spacetime (see Eq. (5.42) and the paragraph after that). The extremal case of $\bar{r}_H = \bar{r}_{\min}$, or equivalently

$$(R_s^2 - Q_b)^4 = 0 \Rightarrow M = \frac{\sqrt{Q_b}}{2G}, \quad (4.39)$$

is a natural limit on the minimum black hole mass. A stability analysis is needed to determine if the black hole remnant is stable. Finally the case of $\bar{r}_H < \bar{r}_{\min}$, or equivalently

$$(R_s^2 - Q_b)^4 < 0 \Rightarrow M < \frac{\sqrt{Q_b}}{2G}, \quad (4.40)$$

where the horizon radius is smaller than the minimum radius of 2-spheres. If it is possible, it would describe a spacetime with no event horizon, where due to the presence of a minimum radius of 2-spheres, it would be a one-way wormhole with an extremal null throat at $\bar{r} = \bar{r}_{\min}$ [43].

To gain insight into the meaning of the M parameter, we calculate the usual geometrical definitions of mass. We first calculate the Komar mass [44] starting from the the surface integral expression [45].

$$M_K(r) = \frac{1}{4\pi G} \int_{\partial\Sigma} d^2x \sqrt{\gamma^{(2)}} n_\mu \sigma_\nu \nabla^\mu K^\nu, \quad (4.41)$$

where n^μ is a unit normal timelike vector to the spacelike hypersurface Σ with constant t , and σ^μ is a unit spacelike normal vector to the 2-spheres which is the boundary of $\partial\Sigma$ at infinity, $\gamma_{ij}^{(2)}$ is the metric of that 2-sphere, and K^ν is the timelike Killing vector of the static spacetime. A unit normal vector v^μ to a hypersurface described by a function $f(x) = C$ with C a constant can be written as

$$v^\mu = \pm \sqrt{\frac{\pm 1}{g^{\alpha\beta} \partial_\alpha f \partial_\beta f}} g^{\mu\nu} \partial_\nu f, \quad (4.42)$$

where the positive signs correspond to a spatial unit vector and negative signs correspond to a timelike unit vector. With a diagonal metric, for a spacelike unit vector σ^μ normal to a surface described by $r = C_1$, we obtain

$$\sigma^\mu = \frac{g^{\mu r}}{\sqrt{g^{rr}}}, \quad (4.43)$$

while for a timelike unit vector normal to a hypersurface $t = C_2$, we get

$$n^\mu = -\frac{g^{\mu t}}{\sqrt{-g^{tt}}}. \quad (4.44)$$

Replacing these together with $K^\mu = (1, 0, 0, 0)$ and $\sqrt{\gamma^{(2)}} = g_{\theta\theta} \sin(\theta)$ inside M_K yields

$$\begin{aligned} M_K &= \frac{r^2}{2G} \left(\frac{1}{\sqrt{\nu}} - \frac{\omega}{\nu} + 2r^6 \frac{\omega}{\rho} \right) \\ &= \frac{r^2}{2G} \left(\frac{1}{\sqrt{r^2 + Q_b}} - \frac{R_s - \sqrt{r^2 + Q_b}}{r^2 + Q_b} + 2r^6 \frac{R_s - \sqrt{r^2 + Q_b}}{r^8 + \frac{1}{4} Q_c R_s^2} \right), \end{aligned} \quad (4.45)$$

where we have defined

$$\omega = R_s - \sqrt{\nu} = R_s - \sqrt{r^2 + Q_b}. \quad (4.46)$$

The asymptotic expansion of M_K as $r \rightarrow \infty$ is

$$M_K(r) = M - \frac{Q_b}{Gr} + \mathcal{O}\left(\frac{1}{r^2}\right), \quad (4.47)$$

from which it is seen that the asymptotic limit of the Kumar mass is actually the parameter M in the metric,

$$\lim_{r \rightarrow \infty} M_K(r) = M. \quad (4.48)$$

Next, we compute the ADM mass [46] using the expression [47]

$$M_{\text{ADM}} = \lim_{r \rightarrow \infty} \bar{M}_{\text{ADM}} = \lim_{r \rightarrow \infty} \frac{1}{16\pi G} \int_{\partial\Sigma} d^2x \sqrt{\gamma^{(2)}} \sigma^i (\bar{\eta}^{jk} \mathcal{D}_k q_{ij} - \mathcal{D}_i (\bar{\eta}^{jk} q_{jk})), \quad (4.49)$$

where \mathcal{D} is the covariant derivative associated with the background metric $\bar{\eta}^{jk}$ which is the flat metric in spherical coordinates in our case, $\sigma^i = \bar{\eta}^{ir} / \sqrt{\bar{\eta}^{rr}} = (1, 0, 0)$ is the unit spacelike normal outward-pointing vector to the 2-sphere $\partial\Sigma$ at infinity, which is the boundary of the spatial hypersurface Σ . Also q_{ij} is the induced metric on the 3D spatial hypersurface Σ , and γ_{ij} is the metric of the 2-sphere $\partial\Sigma$. Using these, we obtain

$$\begin{aligned} \bar{M}_{\text{ADM}} &= \frac{\omega(\rho - 2r^8) - \sqrt{\nu}\rho}{2G\sqrt{\rho}r^3\omega} \\ &= \frac{1}{2Gr^3} \left[\frac{\frac{1}{4}Q_c R_s^2 - r^8}{\sqrt{r^8 + \frac{1}{4}Q_c R_s^2}} - \frac{\sqrt{r^2 + Q_b} \sqrt{r^8 + \frac{1}{4}Q_c R_s^2}}{R_s - \sqrt{r^2 + Q_b}} \right]. \end{aligned} \quad (4.50)$$

The asymptotic expansion for $r \rightarrow \infty$ then reads

$$\bar{M}_{\text{ADM}} = M + \frac{2GM^2}{r} + \frac{M(8G^2M^2 - Q_b)}{2r^2} + \mathcal{O}\left(\frac{1}{r^3}\right), \quad (4.51)$$

from which we can see

$$M_{\text{ADM}} = \lim_{r \rightarrow \infty} \bar{M}_{\text{ADM}} = M. \quad (4.52)$$

Finally we turn our attention to the Hawking quasilocal mass, which for spherical symmetry reduces to the Misner-Sharp-Hernandez (MSH) mass [48, 49] given by

$$\begin{aligned} M_{\text{MSH}}(r) &= \frac{r}{2G} (1 - \nabla^a r \nabla_a r) = \frac{r}{2G} \left(1 - \frac{1}{g_{11}}\right) \\ &= \frac{r}{2G} \left(1 - \left(1 - \frac{R_s}{\sqrt{r^2 + Q_b}}\right) \left(1 + \frac{Q_c R_s^2}{4r^8}\right)^{-1/4}\right). \end{aligned} \quad (4.53)$$

It is also evident that $M_{\text{MSH}}(r) \rightarrow M$ as $r \rightarrow \infty$.

We thus find that the parameter M in our GUP-inspired black hole is the same as the above three masses

$$\lim_{r \rightarrow \infty} \bar{M}_{\text{ADM}}(r) = \lim_{r \rightarrow \infty} M_{\text{MSH}}(r) = \lim_{r \rightarrow \infty} M_{\text{K}}(r) = M. \quad (4.54)$$

4.4 Kretschmann scalar

In addition to the metric, we need to also make sure that the asymptotic limit and asymptotic expansion of the Kretschmann scalar K matches those of the classical Schwarzschild spacetime. The expression for K in terms of the canonical variables is found to be

$$\begin{aligned} K = & \frac{4}{\sqrt{\rho}} \\ & + \frac{4r^4}{\nu^5 \rho^{\frac{9}{2}}} \left\{ \rho^4 (\nu^{3/2} - \nu\omega)^2 + 2\nu\rho^4\omega(\sqrt{\nu} - \omega)r^2 + \rho^4\omega^2r^4 \right. \\ & + 16\nu^3\rho^3\omega(\sqrt{\nu} - \omega)r^6 + 2\nu^2\rho^3(3\sqrt{\nu}\omega - 2\nu + 7\omega^2)r^8 \\ & + 2\nu\rho^3\omega(\omega - 2\sqrt{\nu})r^{10} + 2\nu^4\rho^2\omega(\sqrt{\nu} + 96\omega)r^{12} \\ & + 4\nu^3\rho^2\omega(5\omega - 17\sqrt{\nu})r^{14} + \nu^2\rho^2(-4\sqrt{\nu}\omega + 5\nu - 18\omega^2)r^{16} \\ & \left. - 416\nu^4\rho\omega^2r^{20} + 2\nu^3\rho\omega(29\sqrt{\nu} - 3\omega)r^{22} + 231\nu^4\omega^2r^{28} \right\}, \end{aligned} \quad (4.55)$$

where we have used (4.23), (4.24) and (4.46). The Kretschmann expression (4.55) has all the desired properties. First, the asymptotic limit of the Kretschmann scalar vanishes,

$$\lim_{r \rightarrow \infty} K = 0. \quad (4.56)$$

Second, the asymptotic expansion is

$$K|_{r \rightarrow \infty} = \frac{12R_s^2}{r^6} + \mathcal{O}\left(\frac{1}{r}\right)^7, \quad (4.57)$$

in which the leading term is precisely the Schwarzschild Kretschmann scalar. Third, K is always finite over the entire spacetime $r \in [0, \infty]$. In fact noting

$$\nu(r=0) = \lim_{r \rightarrow 0^+} \nu = Q_b, \quad (4.58)$$

$$\rho(r=0) = \lim_{r \rightarrow 0^+} \rho = \frac{1}{4}Q_c R_s^2, \quad (4.59)$$

$$\omega(r=0) = \lim_{r \rightarrow 0^+} \omega = R_s - \sqrt{\nu(r=0)} = R_s - \sqrt{Q_b}, \quad (4.60)$$

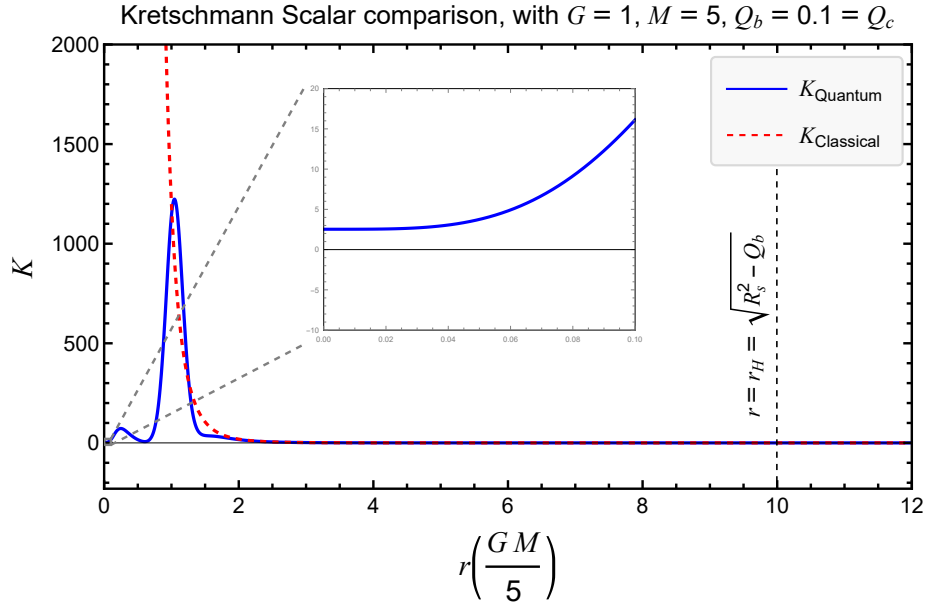


Figure 3. Comparing the classical and effective Kretschmann scalars. In this figure, we have zoomed in on the region where the classical and quantum Kretschmann scalars start to deviate. Notice that a different value of Q_c is used from that in previous plots.

it is rather easy to see from (4.55) that at $r = 0$, which previously exhibited a singularity, we encounter a finite value for the Kretschmann scalar,

$$\lim_{r \rightarrow 0^+} K = K(r = 0) = \frac{4}{\sqrt{\rho}} \Big|_{r=0} = \frac{8}{R_s \sqrt{Q_c}}. \quad (4.61)$$

The finiteness of $K(r = 0)$ was already observed in previous works that only considered the interior [25–28]. This regularity of K is one of the evidences supporting the claim that the singularity of the black hole is resolved in this effective model. The fourth and final property of the Kretschmann expression (4.55), given its denominator and noting the definitions of ν and ρ , ((4.23) and (4.24), respectively), is that K is regular also at the horizon $r = r_H = \sqrt{R_s^2 - Q_b}$, which is another important and desired property. This can be seen explicitly from the values of ν and ρ at the horizon,

$$\nu(r = r_H) = R_s^2, \quad (4.62)$$

$$\rho\nu(r = r_H) = (R_s^2 - Q_b)^4 + \frac{1}{4}Q_c R_s^2. \quad (4.63)$$

Some of the above properties can be directly seen from the plot of the Kretschmann scalar in Fig. 3.

Note that these finite and regular values at the horizon and at $r = 0$ and also the correct asymptotic behavior, are a direct consequence of choosing the signs of the β 's in (4.19)-(4.20), which themselves are the result of the reality condition for the metric.

For completeness, let us also calculate the expansion of the Ricci scalar and Ricci tensor squared in the asymptotic as well as quantum regimes. The asymptotic expressions at spatial infinity read

$$g^{\mu\nu}R_{\mu\nu} = -\frac{2Q_b}{r^4} + \mathcal{O}\left(\frac{1}{r}\right)^5 \quad \text{and} \quad R_{\mu\nu}R^{\mu\nu} = \frac{12Q_b}{r^8} + \mathcal{O}\left(\frac{1}{r}\right)^9. \quad (4.64)$$

In the quantum regime, as $r \rightarrow 0$,

$$g^{\mu\nu}R_{\mu\nu} = \frac{2}{(Q_c R_s^2/4)^{1/4}} \quad \text{and} \quad R_{\mu\nu}R^{\mu\nu} = \frac{2}{(Q_c R_s^2/4)^{1/2}}. \quad (4.65)$$

It is seen that the main deviations from general relativity are dominated by the quantum parameter Q_b and the scalars at $r = 0$ are finite, depending on the Q_c quantum parameter.

4.5 Effective stress-energy tensor

The properties of the effective quantum geometry can be visualized by an effective stress-energy tensor

$$T_{\mu\nu} = \frac{1}{8\pi G}G_{\mu\nu}, \quad (4.66)$$

where $G_{\mu\nu}$ is the Einstein tensor. Let us start by considering a stress-energy tensor that is in the form of an anisotropic perfect fluid

$$T^{\mu\nu} = (\epsilon + p_\theta)U^\mu U^\nu + (p_r - p_\theta)W^\mu W^\nu + p_\theta g^{\mu\nu}, \quad (4.67)$$

characterized by an effective energy density ϵ , and radial and tangential pressure densities p_r and p_θ ($= p_\phi$), respectively. Here U^μ is a unit timelike vector field, $U^\mu U_\mu = -1$, which for a comoving fluid becomes

$$U^\mu = \left(\sqrt{-g^{00}}, 0, 0, 0\right), \quad (4.68)$$

and W^μ is a unit spacelike vector field, $W^\mu W_\mu = 1$, and satisfying $U^\mu W_\mu = 0$. With these conditions, it becomes

$$W^\mu = \left(0, \sqrt{g^{11}}, 0, 0\right). \quad (4.69)$$

Using Einstein's equation we can then write for the exterior

$$\epsilon = -\frac{1}{8\pi G}g^{00}G_{00}, \quad (4.70)$$

$$p_r = \frac{1}{8\pi G}g^{11}G_{11}, \quad (4.71)$$

$$p_\theta = \frac{1}{8\pi G}g^{22}G_{22}. \quad (4.72)$$

For the interior, we need to switch $g^{00} \leftrightarrow g^{11}$ and $G_{00} \leftrightarrow G_{11}$, and hence $\epsilon \leftrightarrow -p_r$. Thus, in the quantum region, $r = 0$, we get

$$\epsilon = \frac{1}{4\sqrt{2}\pi G} \frac{1}{(Q_c R_s^2)^{1/4}}, \quad (4.73)$$

$$p_r = -\frac{1}{4\sqrt{2}\pi G} \frac{1}{(Q_c R_s^2)^{1/4}}, \quad (4.74)$$

$$p_\theta = 0, \quad (4.75)$$

Furthermore, the asymptotic behavior of these quantities at $r \rightarrow \infty$ is

$$\epsilon = \frac{1}{8\pi G} \frac{R_s Q_b}{r^5} + \mathcal{O}\left(\frac{1}{r}\right)^7, \quad (4.76)$$

$$p_r = -\frac{1}{4\pi G} \frac{Q_b}{r^4} + \mathcal{O}\left(\frac{1}{r}\right)^5, \quad (4.77)$$

$$p_\theta = \frac{1}{4\pi G} \frac{Q_b}{r^4} + \mathcal{O}\left(\frac{1}{r}\right)^5. \quad (4.78)$$

The fall-off is as rapid as r^{-4} in which the Schwarzschild spacetime is recovered. The asymptotic behavior is dominated by Q_b and corrections due to Q_c are subdominant.

We can now consider the energy conditions. The weak energy condition is satisfied if $\epsilon \geq 0$ and $\epsilon + p_i \geq 0$ with $i = r, \theta, \phi$, noting that $p_\theta = p_\phi$. The strong energy condition is satisfied if $\epsilon + p_i \geq 0$ and $\epsilon + \sum_i p_i \geq 0$. Finally, the dominant energy condition is satisfied if $\epsilon \geq |p_i|$. From (4.73)-(4.75), we see that at the origin, $r = 0$, the weak, strong and dominant energy conditions are satisfied. However, at $r \rightarrow \infty$, the leading terms of (4.76)-(4.78), violate all energy conditions, although they all vanish at infinity and thus are nonviolating.

We would like to emphasize that these are not (non)violation of an actual matter field energy condition, since this is a vacuum model. One only obtains an stress-energy tensor if one uses the Einstein's equations. However, these are not the equations of motion in our model, since this is a modified theory due to quantum gravity effects. So one should not read too much into the above energy conditions. We have only presented the above results for completeness.

5 Geodesics

Since the metric is static and spherically symmetric, there are three spatial Killing vector fields and one asymptotically timelike one, associated to the rotational symmetry of geodesics and their energy in this spacetime, respectively. Hence, we can fix the direction of the angular momentum ($\theta = \pi/2$) and write its conserved magnitude as

$$L = g_{22} \frac{d\phi}{d\lambda} = \rho^{\frac{1}{4}} \frac{d\phi}{d\lambda}, \quad (5.1)$$

where λ is the affine parameter of the geodesics. In the same way, the conserved energy of the geodesic is

$$E = -g_{00} \frac{dt}{d\lambda} = \sqrt{\frac{\nu}{\sqrt{\rho}}} (\sqrt{\nu} - R_s) \frac{dt}{d\lambda}. \quad (5.2)$$

The conservation of the velocity vector (momentum for null vector) of the geodesic yields

$$\varepsilon = -g_{\mu\nu} \frac{dx^\mu}{d\lambda} \frac{dx^\nu}{d\lambda} = \begin{cases} 0, & \text{null geodesics} \\ 1, & \text{timelike geodesics} \end{cases}. \quad (5.3)$$

Combining these conserved quantities, we obtain in general,

$$-\frac{1}{2} g_{00} g_{11} \left(\frac{dr}{d\lambda} \right)^2 - \frac{1}{2} g_{00} \left[\frac{L^2}{g_{22}} + \varepsilon \right] = \frac{1}{2} E^2, \quad (5.4)$$

which can be written more explicitly in our model as

$$\frac{1}{2} \frac{\nu}{r^2} \left(\frac{dr}{d\lambda} \right)^2 + V_{\text{eff}} = \bar{E}, \quad (5.5)$$

such that the energy is not r dependent. We have defined the effective potential V_{eff} and the energy \bar{E} as

$$V_{\text{eff}} = -\frac{1}{2} g_{00} \left[\frac{L^2}{g_{22}} + \varepsilon \right] = \frac{1}{2} \sqrt{\frac{\nu}{\sqrt{\rho}}} (\sqrt{\nu} - R_s) \left[\frac{L^2}{\rho^{\frac{1}{4}}} + \varepsilon \right], \quad (5.6)$$

$$\bar{E} = \frac{1}{2} E^2. \quad (5.7)$$

Given that ν/r^2 never vanishes in our model, the circular orbits are located at r for which $dV_{\text{eff}}/dr = 0$. Using (5.6) in terms of a general g_{00} and g_{22} , this condition is translated to

$$\varepsilon g_{22}^2 \frac{dg_{00}}{dr} + L^2 \left(g_{22} \frac{dg_{00}}{dr} - g_{00} \frac{dg_{22}}{dr} \right) = 0, \quad (5.8)$$

for a general stationary spherically symmetric metric in diagonal form.

5.1 Null geodesics and the photon sphere

For null geodesics $\varepsilon = 0$ and the condition for the photon sphere(s) from (5.6) and (5.8), we have

$$V_{\text{eff}} = -\frac{1}{2}g_{00} \left[\frac{L^2}{g_{22}} \right] = \frac{1}{2} \sqrt{\frac{\nu}{\sqrt{\rho}}} (\sqrt{\nu} - R_s) \left[\frac{L^2}{\rho^{\frac{1}{4}}} \right], \quad (5.9)$$

$$g_{22} \frac{dg_{00}}{dr} - g_{00} \frac{dg_{22}}{dr} = 0. \quad (5.10)$$

In our model, this last condition yields

$$\frac{1}{2} (1 + \sqrt{\rho}) \frac{1}{\rho} \frac{d\rho}{dr} = \left(1 + \sqrt{\rho} \frac{\sqrt{\nu}}{\sqrt{\nu} - R_s} \right) \frac{1}{\nu} \frac{d\nu}{dr}. \quad (5.11)$$

This equation cannot be solved analytically. But we can obtain important information on how to proceed from the plot of the potential and its derivative that is presented in Fig. 4. From this figure it is evident that for the null case there seems to be only one maximum, i.e., an unstable circular orbit, outside of the black hole. This is similar to the classical case. We see that the position of this photon sphere is very close to the classical photon sphere, which is at $r_{\text{ph}}^{\text{class}} = 3R_s/2$. This observation lets us compute the approximate position of this effective exterior photon sphere. To this end, we first expand dV_{eff}/dr up to first order in Q_b and Q_c . Then expand the resulting expression for $r = 3R_s/2 + \delta r$ with $\delta r \rightarrow 0$ up to the first order in δr . From here we solve this approximate $dV_{\text{eff}}/dr = 0$ for δr and finally expand this δr up to the first order in Q_b and Q_c . The result is the approximate position of the photon sphere given by

$$r_{\text{ph}}^{\text{quat}} = \frac{3R_s}{2} - \frac{7Q_b}{9R_s} + \frac{64Q_c}{6561R_s^5}. \quad (5.12)$$

As expected, the leading correction is only in Q_b , since this is the quantum parameter that is important near the horizon.

5.2 Timelike geodesics

Setting $\varepsilon = 1$ in (5.8) yields the condition for circular orbits in the timelike case:

$$(g_{22} + L^2) g_{22} \frac{dg_{00}}{dr} - L^2 g_{00} \frac{dg_{22}}{dr} = 0. \quad (5.13)$$

This equation is even more complicated than its null counterpart and cannot be solve analytically. Nevertheless, we can again plot the effective potential

$$V_{\text{eff}} = -\frac{1}{2}g_{00} \left[\frac{L^2}{g_{22}} + 1 \right] = \frac{1}{2} \sqrt{\frac{\nu}{\sqrt{\rho}}} (\sqrt{\nu} - R_s) \left[\frac{L^2}{\rho^{\frac{1}{4}}} + 1 \right] \quad (5.14)$$

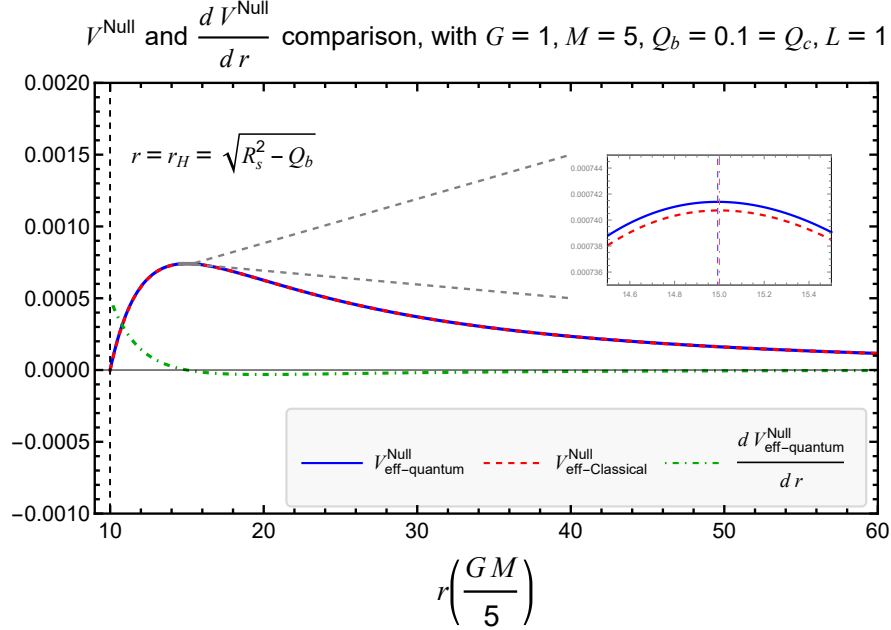


Figure 4. The null effective potential for both the classical and quantum cases, and the derivative of the effective potential in the exterior. It is seen that there seems to be only one extremum in the exterior which is a maximum. This marks the position of the photon sphere. The zoomed-in part shows that the effective photon sphere has a smaller radius (vertical dashed blue line) compared to the classical one (vertical dot dashed red line at $3R_2/2$).

and its derivative. Figure 5 shows the effective potential in the exterior of the black hole. In this region, seemingly there are only two extrema for V_{eff} corresponding to two circular orbits, just as in the classical case. Although the location of these in the quantum black hole are different from the classical ones by a very small amount. This is expected since all our computations until now show that the exterior of this black hole exhibit similar qualitative behaviors as the classical Schwarzschild black hole.

5.3 Painlevé-Gullstrand coordinates and infalling observers

5.3.1 Metric in the Painlevé-Gullstrand coordinates

The Painlevé-Gullstrand (PG) coordinates are derived from the Schwarzschild coordinates by making a coordinate transformation $t \rightarrow t_{\text{PG}}(r, t)$ where t_{PG} is the proper time of the geodesics of an infalling observer with initial zero radial velocity and vanishing angular momentum. This condition means $U^\mu \partial_\mu t_{\text{PG}} = 1$ with $U^\theta = 0 = U^\phi$. Setting

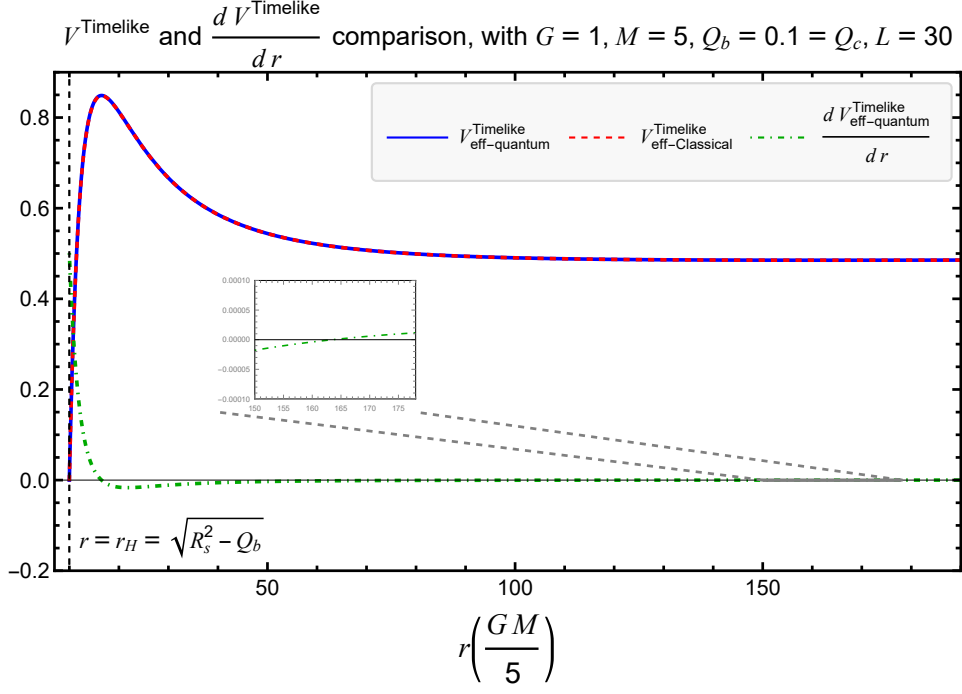


Figure 5. The timelike effective potential for both the classical and quantum cases, and the derivative of the effective potential in the exterior. The quantum curve is qualitatively similar to the classical one where there are two circular orbits in the exterior.

the constants of motion $E = 1$ and $L = 0$, one obtains

$$dt_{\text{PG}} = dt + \sqrt{-g_{11} \left(1 + \frac{1}{g_{00}} \right)} dr \quad (5.15)$$

After this transformation, the metric in the new coordinates is written as

$$ds^2 = g_{00}^{(\text{PG})} dt_{\text{PG}}^2 + 2g_{01}^{(\text{PG})} dt_{\text{PG}} dr + g_{11}^{(\text{PG})} dr^2 + g_{22}^{(\text{PG})} d\Omega^2. \quad (5.16)$$

For our metric, we obtain

$$g_{00}^{(\text{PG})} = g_{00} = -\frac{\sqrt{r^2 + Q_b}}{\left(r^8 + \frac{1}{4} Q_c R_s^2 \right)^{\frac{1}{4}}} \left(\sqrt{r^2 + Q_b} - R_s \right), \quad (5.17)$$

$$g_{01}^{(\text{PG})} = -g_{00} \sqrt{-g_{11} \left(1 + \frac{1}{g_{00}} \right)} = \sqrt{1 + \frac{Q_b}{r^2}} \sqrt{1 - \frac{\sqrt{r^2 + Q_b} \left(\sqrt{r^2 + Q_b} - R_s \right)}{\left(r^8 + \frac{1}{4} Q_c R_s^2 \right)^{\frac{1}{4}}}}, \quad (5.18)$$

$$g_{11}^{(\text{PG})} = -g_{00}g_{11} = 1 + \frac{Q_b}{r^2}, \quad (5.19)$$

$$g_{22}^{(\text{PG})} = g_{22} = \left(r^8 + \frac{1}{4}Q_c R_s^2 \right)^{\frac{1}{4}}. \quad (5.20)$$

This metric can be used to study the behavior of infalling observers crossing the horizon. Notice that the inverse transformation from PG to diagonal in the interior matches precisely the metric (4.15) with componets (4.16)-(4.18), but with t and r switched.

5.3.2 Velocity and proper time of the infalling geodesics

Using PG coordinates, we can compute certain interesting aspects of an infalling observer. We first compute the velocity of the observer falling into the black hole in its own frame (i.e., proper time). For this, we replace the left-hand side of (5.16) with $ds^2 = -d\tau^2$, where τ is the proper time of the infalling observer. We do the same for the right-hand side by replacing $dt_{\text{PG}} = d\tau$. As a result, we obtain

$$-1 = g_{00}^{(\text{PG})} + 2g_{01}^{(\text{PG})} \frac{dr}{d\tau} + g_{11}^{(\text{PG})} \left(\frac{dr}{d\tau} \right)^2, \quad (5.21)$$

with the solution

$$v_{\text{rain}} = \frac{dr}{d\tau} = \frac{-g_{01}^{(\text{PG})} \pm \sqrt{-g_{00}^{(\text{PG})} g_{11}^{(\text{PG})} + \left(g_{01}^{(\text{PG})} \right)^2 - g_{11}^{(\text{PG})}}{g_{11}^{(\text{PG})}}. \quad (5.22)$$

For our metric, both of the above solutions yield

$$v_{\text{rain}} = \frac{dr}{d\tau} = -\frac{r}{\sqrt{\nu}} \sqrt{1 - \frac{\sqrt{\nu}(\sqrt{\nu} - R_s)}{\rho^{\frac{1}{4}}}}. \quad (5.23)$$

In the classical limit $\rho_{\text{class}} = r^8$, and hence the above velocity diverges at $r \rightarrow 0$ as is well-known. However, quantum corrections stop this expression from diverging, since ρ does not vanish in the quantum regime thanks to the presence of a quantum term proportional to Q_c in (4.24). As can be seen from Fig. 6, v_{rain} remains finite within the black hole, and the derivative dv_{rain}/dr changes sign close to $r = 0$, as expected, to keep it from diverging to $-\infty$. Furthermore, in the quantum case, the velocity at $r = 0$ is $v_{\text{rain}}(r = 0) = 0$. From this, it is clear that the deciding factor in non-divergence of the radial infalling velocity is Q_c as expected since as we mentioned before, Q_c governs the important quantum effects close to the $r = 0$ region.

Using (5.23), we also compute the proper time for a typical radially infalling observer. If the observer starts from an initial position r_i , the proper time it takes for it

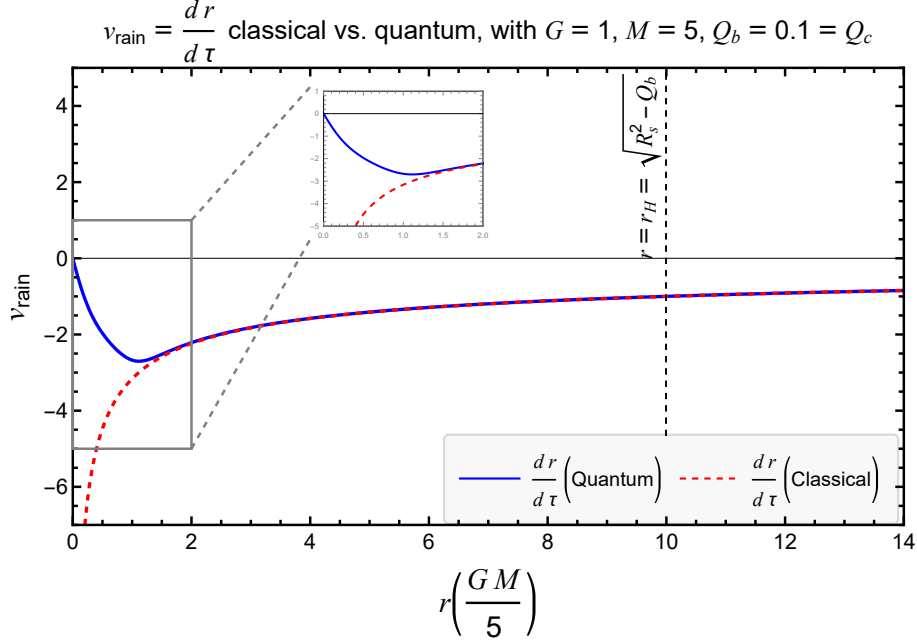


Figure 6. Radial velocity of an infalling observer in Painlevé-Gullstrand coordinates for the classical and quantum cases.

to reach r_f is computed using

$$\Delta\tau = \int_{r_i}^{r_f} \frac{1}{v_{\text{rain}}} dr. \quad (5.24)$$

This integral is quite complicated and cannot be computed analytically. Numerical computations show that this proper time diverges whenever $r_f = 0$. It is because the integrand diverges since, as discussed above, $v_{\text{rain}}(r = 0) = 0$.

One can see this analytically by expanding the integrand up to the first order in Q_b and Q_c and then evaluate the integral. The result is

$$\begin{aligned} \Delta\tau \approx & -\frac{2}{3}r\sqrt{\frac{r}{R_s}} + Q_b\sqrt{\frac{r}{R_s}}\left(\frac{1}{2r} - \frac{1}{R_s}\right) \\ & + \frac{Q_c}{r^5}\sqrt{\frac{R_s}{r}}\left(\frac{1}{208}\frac{R_s}{r} - \frac{1}{176}\right)\Bigg|_{r_i}^{r_f}. \end{aligned} \quad (5.25)$$

The classical limit of this expression matches the classical Schwarzschild black hole. In this limit, the falling observer will reach the singularity located at $r_f = 0$ in a finite proper time. However, in the quantum regime, it takes infinite proper time to reach $r_f = 0$ from any initial point r_i .

5.4 Expansion and Raychaudhuri equation

5.4.1 Expansion tensor and scalar

To obtain the expansion scalar, we first need to find the so-called expansion or deviation tensor. To find this tensor, we consider a congruence of non-affinely parametrized null geodesics with null tangent vectors k^μ such that

$$k_\mu k^\mu = 0 \quad \text{and} \quad k^\mu \nabla_\mu k^\nu = \Omega k^\nu. \quad (5.26)$$

Next, we decompose the spacetime metric $g_{\mu\nu}$ into a longitudinal part and a part $h_{\mu\nu}$ transverse to k^μ . For this, we need to introduce another auxiliary null vector field ℓ^μ such that

$$\ell_\mu \ell^\mu = 0 \quad \text{and} \quad k^\mu \ell_\mu = -1. \quad (5.27)$$

In this way, we can decompose the spacetime metric $g_{\mu\nu}$ as

$$g_{\mu\nu} = h_{\mu\nu} - k_\mu \ell_\nu - k_\nu \ell_\mu, \quad (5.28)$$

where

$$h_{\mu\nu} k^\nu = 0 \quad \text{and} \quad h_{\mu\nu} \ell^\nu = 0. \quad (5.29)$$

The expansion tensor is then expressed as

$$\Theta_{\mu\nu} = h^\alpha{}_\mu h^\beta{}_\nu \nabla_\beta k_\alpha. \quad (5.30)$$

This tensor can be decomposed into its irreducible parts

$$\Theta_{\mu\nu} = \frac{1}{2} \theta h_{\mu\nu} + \sigma_{\mu\nu} + \omega_{\mu\nu}, \quad (5.31)$$

where the trace

$$\theta = g^{\mu\nu} \Theta_{\mu\nu}, \quad (5.32)$$

is the expansion scalar describing the expansion or compression of the cross section of a congruence of null geodesics. The traceless symmetric part

$$\sigma_{\mu\nu} = \Theta_{(\mu\nu)} - \frac{1}{2} \theta h_{\mu\nu}, \quad (5.33)$$

is the shear describing how a circular cross section of the congruence changes its shape, and the antisymmetric part

$$\omega_{\mu\nu} = \Theta_{[\mu\nu]}, \quad (5.34)$$

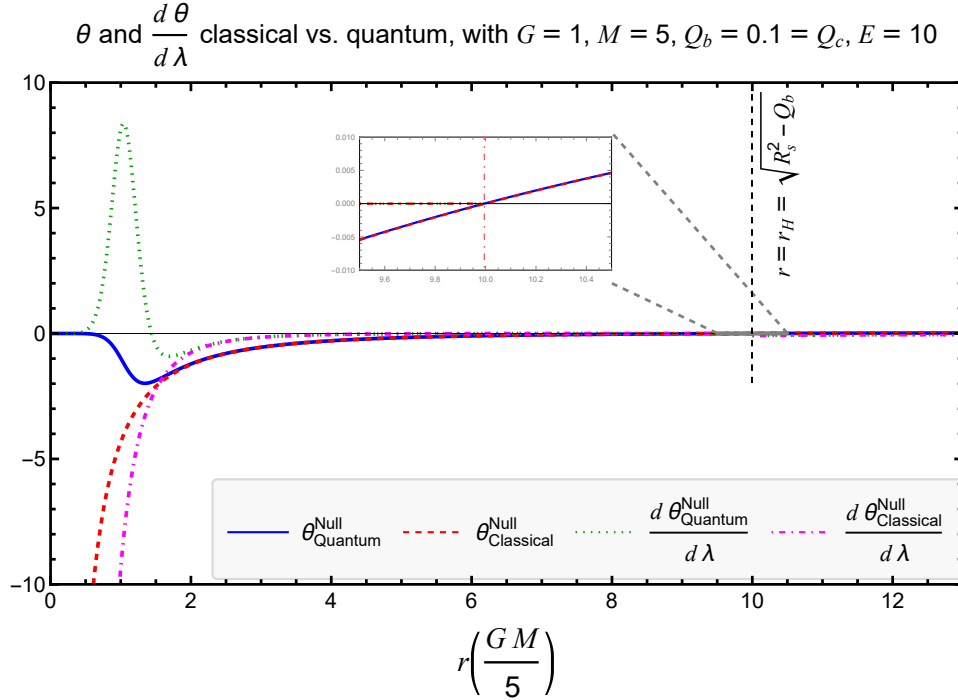


Figure 7. The plot of the outgoing expansion scalar θ_+ and the corresponding Raychaudhuri equation $d\theta_+/d\lambda$ for a congruence of null radial geodesics. It is clear that the quantum versions are finite everywhere particularly at $r = 0$ where they vanish.

is the rotation or vorticity describing how the cross section rotates.

Starting with a null radial congruence described by

$$k^\mu = (k^0, k^1, 0, 0), \quad (5.35)$$

and the auxiliary field

$$\ell^\mu = (\ell^0, \ell^1, 0, 0), \quad (5.36)$$

we can fix k^0 , k^1 and ℓ^1 by demanding the left equation in (5.26) and the two equations in (5.27). In particular the condition $k^\mu k_\mu = 0$ leads to two solutions for k^1 , one corresponding to the outgoing and the other one to the ingoing radial null curves. The component $\ell^0 > 0$ remains arbitrary, and we choose it to be a constant, so that its choice only contributes to an overall scaling of expansion and Raychaudhuri equation.

After this step, one can compute the expansion tensor in the PG coordinates using (5.30). Using that, it is straightforward to compute the expansion, shear and vorticity

using (5.32), (5.33), and (5.34), respectively as

$$\theta_{\pm} = \frac{r^8}{\ell^0 \sqrt{r^2 + Q_b} (r^8 + \frac{1}{4} Q_c R_s^2)} \left(\pm 1 - \sqrt{1 + \frac{\sqrt{r^2 + Q_b} (R_s - \sqrt{r^2 + Q_b})}{(r^8 + \frac{1}{4} Q_c R_s^2)^{\frac{1}{4}}}} \right), \quad (5.37)$$

$$\sigma_{\mu\nu} \sigma^{\mu\nu} = 0, \quad (5.38)$$

$$\omega_{\mu\nu} \omega^{\mu\nu} = 0, \quad (5.39)$$

where $+$ and $-$ correspond to outgoing and ingoing curves, respectively. Notice that $\ell^0 > 0$ is an overall constant. As expected the classical limit, $Q_b \rightarrow 0$ and $Q_c \rightarrow 0$, of the expansion scalar matches that of the classical Schwarzschild black hole in PG coordinates, particularly for $\ell^0 = 1/2$,

$$\theta_{\pm}^{\text{class.}} = \frac{1}{\ell^0 r} \left(\pm 1 - \sqrt{\frac{R_s}{r}} \right). \quad (5.40)$$

We also see that

$$\theta_{\pm}(r=0) = 0. \quad (5.41)$$

This, i.e., θ_{\pm} being finite everywhere, particularly at the location which used to be a singularity at $r=0$, is another strong indication of the resolution of singularity. Also note that at the horizon, we have

$$\theta_{\pm}(r=r_H) = \frac{4(\pm 1 - 1)(Q_b - R_s^2)^4}{\ell^0 R_s [4(Q_b - R_s^2)^4 + Q_c R_s^2]} \quad (5.42)$$

which reduces to the classical expression for $Q_b \rightarrow 0$ and $Q_c \rightarrow 0$. Of particular importance is to notice that while θ_- is always negative (except at $r=0$), the outward expansion θ_+ is positive in the exterior, becomes zero at the horizon $r=r_H$, and is negative in the interior. This shows that the black hole region is a trapped region as expected.

Using $k^1 = dr/d\lambda$ above, where λ is the non-affine parameter of the curves of the null geodesics, one can also integrate for the affine parameter along an infalling null radial geodesic as

$$\Delta\lambda = \int_{r_i}^{r_f} \frac{1}{k^1(r)} dr. \quad (5.43)$$

This can be computed numerically and shows that it will diverge. Furthermore, a plot of $1/k^1$ itself shows that it diverges at $r=0$.

5.4.2 Raychaudhuri equation

The Raychaudhuri equation describes the evolution of the expansion scalar in terms of the affine parameter of the geodesics. For a null congruence we have

$$\frac{d\theta}{d\lambda} = -\frac{1}{2}\theta^2 - \sigma_{\mu\nu}\sigma^{\mu\nu} + \omega_{\mu\nu}\omega^{\mu\nu} - R_{\mu\nu}k^\mu k^\nu. \quad (5.44)$$

If we were considering the classical regime, clearly the last term related to the null energy condition would have vanished due to the fact that we are in vacuum. However, in the effective regime, the equations of motion are not Einstein's equations and hence we will not have $R_{\mu\nu} = 0$ necessarily. In this regime, the Raychaudhuri equation becomes

$$\frac{d\theta_\pm}{d\lambda} = \frac{r^8 \left(r^{10} - \frac{7}{4}Q_c R_s^2 r^2 - 2Q_c Q_b R_s^2 \right)}{(r^2 + Q_b)^2 \left(r^8 + \frac{1}{4}Q_c R_s^2 \right)^2 (\ell^0)^2} \times \left[\pm \sqrt{1 + \frac{\sqrt{r^2 + Q_b} \left(R_s - \sqrt{r^2 + Q_b} \right)}{\left(r^8 + \frac{1}{4}Q_c R_s^2 \right)^{1/4}} - \frac{\sqrt{r^2 + Q_b} \left(R_s - \sqrt{r^2 + Q_b} \right)}{2 \left(r^8 + \frac{1}{4}Q_c R_s^2 \right)^{1/4}}} - 1 \right] \quad (5.45)$$

This expression never diverges and in particular becomes zero at $r = 0$. Furthermore, the classical limit of this expression yields

$$\frac{d\theta_\pm}{d\lambda} = \frac{1}{2r^3 (\ell^0)^2} \left[\pm 2 \sqrt{r R_s} - r - R_s \right] \quad (5.46)$$

which clearly diverges at $r \rightarrow 0$.

A plot of both θ_+ and $d\theta_+/d\lambda$ for outgoing rays is presented in Fig. 7. The regularity of both θ and $d\theta/d\lambda$ was also observed before in the models that only considered the interior [25–28].

The finiteness, and in fact vanishing, of both null θ_\pm and $d\theta_\pm/d\lambda$ over the entire spacetime, together with regularity of the Kretschmann scalar everywhere in this spacetime indicates that the singularity is resolved in this quantum black hole model.

6 Discussion and conclusions

In this work, we have examined whether one can analytically continue the interior metric of a GUP-inspired black hole introduced earlier [25] to the full spacetime, via switching the radial spacelike and the timelike coordinates $t \leftrightarrow r$. This would be similar to the classical Schwarzschild case where one can simply obtain the interior from the

exterior, and vice versa, in this way. Our analysis showed that the resulting extended metric and consequently the Kretschmann scalar have serious issues in the asymptotic $r \rightarrow \infty$ region: g_{00} will not be in the desired form and the Kretschmann scalar will fall off as r^{-4} instead of r^{-6} . This issue is similar to the case of [37, 38].

In order to remedy these issues, we have introduced an improved scheme, borrowed from the techniques used in loop quantum gravity, whereby one makes the previously constant quantum parameters of the model momentum-dependent. In this specific model, the minimal uncertainty parameters are β_b and β_c , and we modify them to $\bar{\beta}_b = \beta_b L_0^4 / p_b^2$ and $\bar{\beta}_c = \beta_c L_0^4 / p_c^2$, where p_b and p_c are momenta of the theory which correspond to the components of the densitized triads; essentially the components of the metric. Remarkably, this rather simple prescription, not only results in all the desired asymptotic behaviors, but also renders the black hole regular. Furthermore, the Kretschmann scalar vanishes at $r \rightarrow \infty$ as in the classical case, and more importantly its expansion up to zero'th order in quantum parameters exactly matches that of the Schwarzschild metric. In addition, all the classical limits ($\beta_b \rightarrow 0$ and $\beta_c \rightarrow 0$) match the classical Schwarzschild spacetime.

We find that in order for the metric components to always remain real, β_b and β_c should be negative. This is the same result that was previously obtained if one wants to resolve the singularity [25]. In this work, this condition is derived more systematically and is much stronger (demanding metric reality and not finiteness of the Kretschmann scalar). The condition then leads directly to the resolution of the singularity by rendering the denominator of the Kretschmann scalar positive and nonzero for any value of the radial coordinate r , including the horizon.

In Schwarzschild coordinates in which the metric function $g_{22} = \bar{r}^2$ for some \bar{r} coordinate, we find a minimum mass-dependent size of 2-spheres given by quantum parameter Q_c , while the other quantum parameter Q_b is responsible for quantum effects near the horizon.

Finally, we computed the null expansion and the Raychaudhuri equation for a congruence of null geodesics and show that they both are regular everywhere in this spacetime, which together with regularity of the Kretschmann scalar, indicates that the singularity is resolved in this quantum black hole spacetime.

Acknowledgments

The authors acknowledge the support of the Natural Sciences and Engineering Research Council of Canada (NSERC). Nous remercions le Conseil de recherches en sciences naturelles et en génie du Canada (CRSNG) de son soutien.

A Equations of motion of the interior

Given the classical equations of motion ($i = b, c$)

$$\dot{q}_i = \{q_i, H\}_{\text{cl.}}, \quad \dot{p}_i = \{p_i, H\}_{\text{cl.}}, \quad (\text{A.1})$$

using the classical Poisson brackets (2.4), if the classical algebra change to the modified algebra as

$$\{q_i, p_j\}_{\text{eff.}} = \{q_i, p_j\}_{\text{cl.}} (1 + F(q, p, \beta_i)) \delta_{ij}, \quad (\text{A.2})$$

the new equations of motion become

$$\dot{q}_i = \{q_i, H\}_{\text{eff.}} = \{q_i, H\}_{\text{cl.}} (1 + F(q, p, \beta_i)), \quad \dot{p}_i = \{p_i, H\}_{\text{eff.}} = \{p_i, H\}_{\text{cl.}} (1 + F(q, p, \beta_i)). \quad (\text{A.3})$$

For the non-improved interior case where the solutions are Eqs. (3.6)-(3.9), these EoM are

$$\dot{\tilde{b}} = -\frac{\tilde{b}^2 + \gamma^2}{2\tilde{b}} (1 + \beta_b \tilde{b}^2), \quad (\text{A.4})$$

$$\dot{\tilde{p}}_b = \frac{\tilde{p}_b (\tilde{b}^2 - \gamma^2)}{2\tilde{b}^2} (1 + \beta_b \tilde{b}^2), \quad (\text{A.5})$$

$$\dot{\tilde{c}} = -2\tilde{c} (1 + \beta_c \tilde{c}^2), \quad (\text{A.6})$$

$$\dot{\tilde{p}}_c = 2\tilde{p}_c (1 + \beta_c \tilde{c}^2). \quad (\text{A.7})$$

For the improved interior whose solutions are presented in (4.5)-(4.8), the corresponding EoM are

$$\dot{b} = -\frac{b^2 + \gamma^2}{2b} \left(1 + \frac{\beta_b L_0^4}{p_b^2} b^2\right), \quad (\text{A.8})$$

$$\dot{p}_b = \frac{p_b (b^2 - \gamma^2)}{2b^2} \left(1 + \frac{\beta_b L_0^4}{p_b^2} b^2\right), \quad (\text{A.9})$$

$$\dot{c} = -2c \left(1 + \frac{\beta_c L_0^4}{p_c^2} c^2\right), \quad (\text{A.10})$$

$$\dot{p}_c = 2p_c \left(1 + \frac{\beta_c L_0^4}{p_c^2} c^2\right). \quad (\text{A.11})$$

References

- [1] A. Addazi et al., *Quantum gravity phenomenology at the dawn of the multi-messenger era—A review*, *Prog. Part. Nucl. Phys.* **125** (2022) 103948 [2111.05659].

- [2] LISA collaboration, *New horizons for fundamental physics with LISA*, *Living Rev. Rel.* **25** (2022) 4 [2205.01597].
- [3] LISA COSMOLOGY WORKING GROUP collaboration, *Cosmology with the Laser Interferometer Space Antenna*, *Living Rev. Rel.* **26** (2023) 5 [2204.05434].
- [4] R. Alves Batista et al., *White Paper and Roadmap for Quantum Gravity Phenomenology in the Multi-Messenger Era*, 2312.00409.
- [5] T. Thiemann, *Modern Canonical Quantum General Relativity*, Cambridge Monographs on Mathematical Physics. Cambridge University Press, 2007, 10.1017/CBO9780511755682.
- [6] A. Ashtekar and M. Bojowald, *Quantum geometry and the Schwarzschild singularity*, *Class. Quant. Grav.* **23** (2006) 391 [gr-qc/0509075].
- [7] Böhmer, Christian G. and Vandersloot, Kevin, *Loop Quantum Dynamics of the Schwarzschild Interior*, *Phys. Rev. D* **76** (2007) 104030 [0709.2129].
- [8] D.-W. Chiou, *Phenomenological loop quantum geometry of the Schwarzschild black hole*, *Phys. Rev. D* **78** (2008) 064040 [0807.0665].
- [9] H. A. Morales-Técotl, S. Rastgoo and J. C. Ruelas, *Effective dynamics of the Schwarzschild black hole interior with inverse triad corrections*, *Annals Phys.* **426** (2021) 168401 [1806.05795].
- [10] K. Blanchette, S. Das, S. Hergott and S. Rastgoo, *Black hole singularity resolution via the modified Raychaudhuri equation in loop quantum gravity*, *Phys. Rev. D* **103** (2021) 084038 [2011.11815].
- [11] J. G. Kelly, R. Santacruz and E. Wilson-Ewing, *Effective loop quantum gravity framework for vacuum spherically symmetric space-times*, 2006.09302.
- [12] R. Gambini, J. Olmedo and J. Pullin, *Spherically symmetric loop quantum gravity: analysis of improved dynamics*, *Class. Quant. Grav.* **37** (2020) 205012 [2006.01513].
- [13] A. Ashtekar, J. Olmedo and P. Singh, *Quantum Transfiguration of Kruskal Black Holes*, *Phys. Rev. Lett.* **121** (2018) 241301 [1806.00648].
- [14] N. Bodendorfer, F. M. Mele and J. Münch, *(b,v)-Type Variables for Black to White Hole Transitions in Effective Loop Quantum Gravity*, 1911.12646.
- [15] L. Modesto, *Semiclassical loop quantum black hole*, *Int. J. Theor. Phys.* **49** (2010) 1649 [0811.2196].
- [16] M. Bojowald, *Black-Hole Models in Loop Quantum Gravity*, *Universe* **6** (2020) 125 [2009.13565].
- [17] R. Gambini, J. Pullin and S. Rastgoo, *New variables for 1+1 dimensional gravity*, *Class. Quant. Grav.* **27** (2010) 025002 [0909.0459].

- [18] A. Corichi, A. Karami, S. Rastgoo and T. Vukašinac, *Constraint Lie algebra and local physical Hamiltonian for a generic 2D dilatonic model*, *Class. Quant. Grav.* **33** (2016) 035011 [[1508.03036](#)].
- [19] A. Corichi, J. Olmedo and S. Rastgoo, *Callan-Giddings-Harvey-Strominger vacuum in loop quantum gravity and singularity resolution*, *Phys.Rev.D* **94** (2016) 084050 [[1608.06246](#)].
- [20] A. Ashtekar, S. Fairhurst and J. L. Willis, *Quantum gravity, shadow states, and quantum mechanics*, *Class. Quant. Grav.* **20** (2003) 1031 [[gr-qc/0207106](#)].
- [21] H. A. Morales-Técotl, S. Rastgoo and J. C. Ruelas, *Path integral polymer propagator of relativistic and nonrelativistic particles*, *Phys.Rev.D* **95** (2017) 065026 [[1608.04498](#)].
- [22] H. A. Morales-Técotl, D. H. Orozco-Borunda and S. Rastgoo, *Polymer quantization and the saddle point approximation of partition functions*, *Phys.Rev.D* **92** (2015) 104029 [[1507.08651](#)].
- [23] A. Kempf, G. Mangano and R. B. Mann, *Hilbert space representation of the minimal length uncertainty relation*, *Phys. Rev. D* **52** (1995) 1108 [[hep-th/9412167](#)].
- [24] P. Bosso, G. G. Luciano, L. Petruzzello and F. Wagner, *30 years in: Quo vadis generalized uncertainty principle?*, *Class. Quant. Grav.* **40** (2023) 195014 [[2305.16193](#)].
- [25] P. Bosso, O. Obregón, S. Rastgoo and W. Yupanqui, *Deformed algebra and the effective dynamics of the interior of black holes*, *Class. Quant. Grav.* **38** (2021) 145006 [[2012.04795](#)].
- [26] K. Blanchette, S. Das and S. Rastgoo, *Effective GUP-modified Raychaudhuri equation and black hole singularity: four models*, *JHEP* **09** (2021) 062 [[2105.11511](#)].
- [27] S. Rastgoo and S. Das, *Probing the Interior of the Schwarzschild Black Hole Using Congruences: LQG vs. GUP*, *Universe* **8** (2022) 349 [[2205.03799](#)].
- [28] P. Bosso, O. Obregón, S. Rastgoo and W. Yupanqui, *Black hole interior quantization: a minimal uncertainty approach*, [2310.04600](#).
- [29] G. Lambiase and F. Scardigli, *Lorentz violation and generalized uncertainty principle*, *Phys. Rev. D* **97** (2018) 075003 [[1709.00637](#)].
- [30] F. Scardigli and R. Casadio, *Gravitational tests of the Generalized Uncertainty Principle*, *Eur. Phys. J. C* **75** (2015) 425 [[1407.0113](#)].
- [31] R. Casadio, A. Giugno and A. Giusti, *Global and Local Horizon Quantum Mechanics*, *Gen. Rel. Grav.* **49** (2017) 32 [[1605.06617](#)].
- [32] P. Jizba, H. Kleinert and F. Scardigli, *Uncertainty Relation on World Crystal and its Applications to Micro Black Holes*, *Phys. Rev. D* **81** (2010) 084030 [[0912.2253](#)].

- [33] B. J. Carr, J. Mureika and P. Nicolini, *Sub-Planckian black holes and the Generalized Uncertainty Principle*, *JHEP* **07** (2015) 052 [[1504.07637](#)].
- [34] Y. C. Ong, *Generalized Uncertainty Principle, Black Holes, and White Dwarfs: A Tale of Two Infinities*, *JCAP* **09** (2018) 015 [[1804.05176](#)].
- [35] L. Buoninfante, G. G. Luciano and L. Petrucciello, *Generalized Uncertainty Principle and Corpuscular Gravity*, *Eur. Phys. J. C* **79** (2019) 663 [[1903.01382](#)].
- [36] L. Modesto, *Loop quantum black hole*, *Class. Quant. Grav.* **23** (2006) 5587 [[gr-qc/0509078](#)].
- [37] A. Ashtekar and J. Olmedo, *Properties of a recent quantum extension of the Kruskal geometry*, *Int. J. Mod. Phys. D* **29** (2020) 2050076 [[2005.02309](#)].
- [38] M. Bouhmadi-López, S. Brahma, C.-Y. Chen, P. Chen and D.-h. Yeom, *Asymptotic non-flatness of an effective black hole model based on loop quantum gravity*, *Phys. Dark Univ.* **30** (2020) 100701 [[1902.07874](#)].
- [39] R. Rashidi, *Generalized uncertainty principle and the maximum mass of ideal white dwarfs*, *Annals Phys.* **374** (2016) 434 [[1512.06356](#)].
- [40] A. Mathew and M. K. Nandy, *Existence of Chandrasekhar's limit in GUP white dwarfs*, [2002.08360](#).
- [41] A. Ashtekar, T. Pawłowski and P. Singh, *Quantum Nature of the Big Bang: Improved dynamics*, *Phys. Rev.* **D74** (2006) 084003 [[gr-qc/0607039](#)].
- [42] D.-W. Chiou, W.-T. Ni and A. Tang, *Loop quantization of spherically symmetric midisuperspaces and loop quantum geometry of the maximally extended Schwarzschild spacetime*, [1212.1265](#).
- [43] A. Simpson and M. Visser, *Black-bounce to traversable wormhole*, *JCAP* **02** (2019) 042 [[1812.07114](#)].
- [44] A. Komar, *Positive-definite energy density and global consequences for general relativity*, *Phys. Rev.* **129** (1963) 1873.
- [45] S. M. Carroll, *Spacetime And Geometry An Introduction To General Relativity*. Addison Wesley, 2004.
- [46] R. Arnowitt, S. Deser and C. W. Misner, *Dynamical structure and definition of energy in general relativity*, *Phys. Rev.* **116** (1959) 1322.
- [47] E.ourgoulhon, *3+1 formalism and bases of numerical relativity*, [gr-qc/0703035](#).
- [48] C. W. Misner and D. H. Sharp, *Relativistic equations for adiabatic, spherically symmetric gravitational collapse*, *Phys. Rev.* **136** (1964) B571.
- [49] V. Faraoni, A. Giusti and T. F. Bean, *Asymptotic flatness and Hawking quasilocal mass*, *Phys. Rev. D* **103** (2021) 044026 [[2010.00069](#)].